North Atlantic circulation and reservoir age changes over the past 41,000 years

Auxiliary material

Joseph V. Stern and Lorraine E. Lisiecki

Department of Earth Science, University of California, Santa Barbara, California, USA.

1. Nomenclature: Heinrich Stadial 1 and the Mystery Interval

The term "Heinrich stadial" was originally defined as any cold interval in Greenland that contains a Heinrich event [*Barker et al.*, 2009]. With this definition, the ends of Heinrich stadials are easily identified by rapid warming events in Greenland, but their beginnings are more difficult to identify. For example, recent studies have discussed the beginning of Heinrich Stadial 1 (HS1) as early as 19 kyr BP [*Bouimetarhan et al.*, 2012] or as late as 17 kyr BP [*Thornalley et al.*, 2010b]. For the purposes of this paper, we demarcate the beginning of HS1 as the well-dated 19 kyr BP initiation of deglacial melting [*Clark et al.*, 2009], which also corresponds approximately with the increase in high-latitude North Atlantic (HLNA) reservoir age. Thus, the end of the Last Glacial Maximum (LGM; 26 to 19 kyr BP) [*Clark et al.*, 2009] transitions directly into HS1 (19 to 14.7 kyr BP).

The "Mystery Interval" is often defined by a rapid, large decrease in atmospheric $\Delta^{14}C$ between 17.5 and 14.5 kyr BP and is sometimes used synonymously with HS1 [*Denton et al.*, 2006, 2010; *Broecker and Barker*, 2007; *Broecker et al.*, 2009]. New calibration data [*Ramsey et al.*, 2012; *Southon et al.*, 2012] suggest that this drop began earlier and was not as rapid as previously thought, consistent with a 19 kyr BP start to both the Mystery Interval and HS1.

2. Methods background

The most direct approaches to determining past reservoir ages involve comparing ^{14}C dates from paired terrestrial and marine archives of the same calendar age. For example, the difference between marine and terrestrial uncalibrated ^{14}C ages taken near the same ash layer provides a reservoir age [*Bard et al.*, 1994; *Thornalley et al.*, 2011a]. Alternatively, both marine and terrestrial material can be found in the same sediment core in certain near-shore environments [*Bondevik et al.*, 2006]. In these scenarios, calendar ages can be ascribed either by calibrating terrestrial ^{14}C ages or by deferring to an event age in a Greenland ice core chronology. Complications with these methods include potential bioturbation of sediments, interpolation and the assumption of constant sedimentation rate between dates, and imperfections in ice core chronologies. The most important limitation with these techniques, however, is that they can only be applied to very specific locations and times.

To overcome these limitations, we developed a method (see Methods section below) to reconstruct average HLNA reservoir ages for the past 41 kyr based on four main assumptions: (1) synchrony of benthic $\delta^{18}O$ changes within the deep North Atlantic; (2) synchrony of ice-rafted debris (IRD) deposition within the North Atlantic; (3) synchrony of relative paleointensity (RPI) changes on the Iberian Margin, and; (4) constant low-latitude reservoir ages. Before detailing our methods, we address the validity of each of these assumptions.

3. Deep North Atlantic benthic $\delta^{18}O$ synchrony

The oxygen isotopic composition ($\delta^{18}O$) of benthic foraminiferal calcite is affected by temperature-dependent fractionation and seawater $\delta^{18}O$. The controls on seawater $\delta^{18}O$ can be bifurcated into global effects due to continental ice volume and regional/local effects that covary with salinity. *Shackleton* [1967] laid the foundation for benthic $\delta^{18}O$ stratigraphy by highlighting continental ice volume as the dominant control on glacial-interglacial benthic $\delta^{18}O$ changes. Since then, the assumption of global benthic $\delta^{18}O$ synchrony has been widely employed for the development of both millennial- and orbital-scale chronostratigraphies [e.g., *Pisias et al.*, 1984; *Martinson et al.*, 1987; *Lisiecki and Raymo*, 2005].

A few studies have identified regional differences in the timing of benthic $\delta^{18}O$ changes during the last deglaciation when comparing Atlantic and Pacific [*Skinner and Shackleton*, 2005; *Lisiecki and Raymo*, 2009], intermediate and deep [*Labeyrie et al.*, 2005; *Waelbroeck et al.*, 2011], and North and South Atlantic sites [*Waelbroeck et al.*, 2011]. There is active debate about whether these differences represent diachronous temperature responses [*Skinner and Shackleton*, 2005], slow mixing of the global deglacial $\delta^{18}O$ signal [*Friedrich and Timmermann*, 2012], or changes in water mass properties [*Waelbroeck et al.*, 2011]. No study has observed differences in the timing of benthic $\delta^{18}O$ changes within the deep North Atlantic.

Several model results have addressed the possibility of a diachronous deglacial $\delta^{18}O$ signal within the deep North Atlantic. For the injection of a passive tracer into the HLNA, *Wunsch and Heimbach* [2008] concluded that, "Within the North Atlantic itself, hundreds of years are required to achieve local equilibrium at depth." Tracer injection into a different region would only slightly increase the time to equilibrium in the deep North Atlantic [*Wunsch and Heimbach*, 2008]. *Primeau and Deleersnijder* [2009] point out that *Wunsch and Heimbach* [2008] overestimated equilibrium times by prescribing surface concentrations rather than fluxes of the tracer. This point is conceded by *Siberlin and Wunsch* [2011], but there is some disagreement about the magnitude of this overestimation. These three studies [*Wunsch and Heimbach*, 2008; *Primeau and Deleersnijder*, 2009; *Siberlin and Wunsch*, 2011] are based on present day ocean circulation models that do not fully capture Antarctic Bottom Water (AABW) formation processes, so equilibrium times for tracer injections through AABW are likely overestimated [*Wunsch and Heimbach*, 2008]. AABW was probably the dominant water mass in the deep Atlantic during the LGM and HS1 [*Curry and Oppo*, 2005; *Negre et al.*, 2010]. *Friedrich and Timmermann* [2012] suggest that the time to equilibrium in the deep North Atlantic for a passive tracer injected at the surface HLNA is several thousand years when the AMOC is reduced, but tracer concentrations remain similar within the entire deep North Atlantic as equilibrium is achieved. All these modeling studies treat $\delta^{18}O$ as a purely passive tracer, which could result in slightly overestimated equilibrium times because $\delta^{18}O$ is associated with both temperature and salinity [*Siberlin and Wunsch*, 2011]. Taken together, these modeling results suggest that possible diachroneity of the deglacial $\delta^{18}O$ signal is probably less than a few hundred years (and almost certainly less than 1000 yr) for individual sites in the deep North Atlantic. Our averaging techniques would further minimize the effects of these small diachroneities. The spatial pattern of these diachroneities would probably be complex, as it would depend on the details of bathymetry and deep water flow paths.

We selected an upper boundary of 2000 m water depth for the deep North Atlantic (Figure S1), based on the traditional LGM boundary between Glacial North Atlantic Intermediate Water and Glacial Antarctic Bottom Water [*Curry and Oppo*, 2005], recognizing that many aspects of LGM ocean circulation are unresolved. For example, the LGM boundary between northern- and southern-sourced waters may have been somewhat deeper and the deep Atlantic may have included a third water mass [*Yu et al.*, 2008; *Lippold et al.*, 2012]. The deepest core in our compilation comes from approximately 4600 m. *Waelbroeck et al.* [2011] found that the initial deglacial benthic $\delta^{18}O$ decrease occurred ~500 yr earlier at intermediate depths (1000-2200 m) compared to deep (3000-4100 m) sites within the North Atlantic. However, we find North Atlantic cores from 2000-2200 m consistent with deeper cores.

We chose meridional limits for this study at the equator and 65°N. North and South Atlantic benthic $\delta^{18}O$ changes are often considered synchronous even at the millennial-scale [*Vidal et al.*, 1999]. However, we used a more conservative southern boundary because *Waelbroeck et al.* [2011] identified a ~1000 yr difference between deglacial benthic $\delta^{18}O$ changes when comparing two deep cores from the North and South Atlantic. Our northern boundary at 65°N excludes sites from the Nordic and Arctic Seas and effectively restricts our study area to south of Iceland. Benthic $\delta^{18}O$ from the Nordic and Arctic Seas may record strong local effects [*Meland et al.*, 2008], negating their usefulness for alignments to cores from the open North Atlantic. These extremely high latitude areas probably also experienced variable reservoir ages during the deglaciation [*Voelker et al.*, 1998; *Sarnthein et al.*, 2007; *Hanslik et al.*, 2010], but, again, local overprints may be strong.

The boundary between high and low latitudes was placed at 40°N for our study. This approximates the classical position of the LGM polar front, which was both more southerly and zonal than modern [*Ruddiman and McIntyre*, 1981]. A more recent study suggests that, at least on the Iberian Margin, the polar front may have only reached 40°N during Heinrich events [*Eynaud et al.*, 2009]. Other studies have hypothesized [*Bard*, 1988; *Bard et al.*, 1994] and observed [*Waelbroeck et al.*, 2001] that significant deglacial reservoir age variability is restricted to >40°N in the North Atlantic. Our results are only minimally affected by small shifts in the latitude used for this boundary. Meridional and zonal gradients in reservoir ages within the HLNA are likely to have been present in the past, but the available data do not allow us to identify any spatial variability within the HLNA (see Section 11 of the auxiliary materials for further discussion).

4. Synchrony of ice-rafted debris deposition

North Atlantic IRD correlations are another well-established stratigraphic tool [*Chapman and Shackleton*, 1998; *Elliot et al.*, 2002; *Gherardi et al.*, 2009]. IRD is generally defined as sediment transported to the open ocean by floating icebergs or sea ice that is then deposited upon melting [*Hemming*, 2004]. North Atlantic IRD records are dominated by six prominent peaks during the last glacial period [*Heinrich*, 1988], termed "Heinrich layers" or "Heinrich events" and labeled 1-6 from youngest to oldest. A host of geochemical studies have shown that Heinrich events 1, 2, 4, and 5 were derived from melting of the Laurentide ice sheet through the Hudson Strait; the smaller Heinrich events 3 and 6 record mostly European ice sheet melting and may be affected by low foraminifera intervals (see review by *Hemming* [2004]). In addition to the six Heinrich events (only four of which occur during our study interval), minor IRD peaks have also been used for correlations [*Elliot et al.*, 2002].

"Precursor events" are potentially the biggest threat to accurate IRD correlations. Precursor events refer to IRD deposited immediately before a Heinrich event, identified by distinct lithological and/or geochemical characteristics. For example, the main Hudson Strait Heinrich events are dominated by maxima in detrital carbonate content, while volcanic fragments are a commonly identified precursor [*Bond and Lotti*, 1995; *Hemming*, 2004; *Jullien et al.*, 2006]. The provenance of precursor IRD can be difficult to identify with certainty, and the magnitude of an IRD event at a particular core location depends on both its proximity to the source and additional oceanographic factors [*Hemming*, 2004]. It is thus conceivable to erroneously align precursor IRD with Heinrich event IRD, which would result in age discrepancies of up to ~1000 yr. We paid close attention to additional lithological and geochemical constraints provided by previous authors to avoid naïve IRD alignments for the records we used.

Chapman et al. [2000] proposed that Heinrich Event 1 IRD was deposited ~500 yr earlier in the central Atlantic (40°N) than on the Iberian Margin (38°N). However, the central Atlantic sites they consider are located just north of 40°N, and applying our increased early HS1 reservoir ages would eliminate this IRD age difference. The distinction between precursory IRD beginning at 18 kyr BP, the Laurentide-sourced Heinrich Event 1 peak at 17 kyr BP, and a later European-sourced IRD peak at 16 kyr BP (discussed in the main text) could also influence the conclusions of *Chapman et al.* [2000]. Some of the records used by *Chapman et al.* [2000] are included in our compilation.

5. Iberian Margin relative paleointensity

RPI records characterize changes in the intensity of Earth's magnetic field and have been used for both regional- [*Laj et al.*, 2000; *Thouveny et al.*, 2004] and global-scale correlations [*Laj et al.*, 2004; *Channell et al.*, 2009]. Major events such as the Laschamp (~41 kyr BP) and Mono Lake (~34 kyr BP) excursions provide the most reliable alignment constraints, but all the studies cited above correlate continuous time series.

Iberian Margin RPI records agree quite well with each other, justifying their use as a stratigraphic tool [*Thouveny et al.*, 2004], but we chose not to align North Atlantic RPI records from outside the Iberian Margin. The Laschamp excursion appears to be somewhat broader and occurs somewhat earlier in Iberian Margin records [*Thouveny et al.*, 2004] compared to other North Atlantic records [*Laj et al.*, 2000]. Furthermore, the Mono Lake excursion is difficult to identify in Iberian Margin records, where two or three RPI minima often occur between about 34-39 kyr BP.

Within our compilation of cores that have both benthic $\delta^{18}O$ and planktonic ^{14}C dates, there are more RPI records from the Iberian Margin than from other North Atlantic sites. Therefore, we used Iberian Margin RPI to further constrain our alignments while taking the conservative approach of not including RPI from other North Atlantic sites because Iberian Margin RPI may have some unique features. For our RPI proxy, we used the natural remanent magnetization normalized by the anhysteretic remanent magnetization for the 30 mT alternating field demagnetization step.

6. Low-latitude North Atlantic reservoir ages

In the modern North Atlantic, reservoir ages are 300-400 ^{14}C yr in the tropics and subtropics and 400-500 ^{14}C yr at high latitudes [*Bard*, 1988]. Low-latitude sites are located far from deep water formation regions and their associated upwelling zones, and are isolated from even the most extreme shifts in the polar front, so large reservoir age changes in the past are unlikely. Attention on low-latitude North Atlantic reservoir ages has been disproportionately focused on two regions – the western subtropical Atlantic and the Iberian Margin – because ^{14}C ages from these areas have been included in some calibration curves.

Within the western subtropical Atlantic, the assumption of constant ~400 ^{14}C yr reservoir ages in the Cariaco Basin (11°N) [*Hughen et al.*, 2006] and at Barbados (13°N) [*Fairbanks et al.*, 2005] has generated significant interest. Several studies have now suggested a significant decrease in western subtropical Atlantic reservoir ages during the early Younger Dryas (YD), to values around 200 ^{14}C yr [*Kromer et al.*, 2004; *Ritz et al.*, 2008; *Singarayer et al.*, 2008; *Southon et al.*, 2012]. Another decrease, possibly to reservoir ages as low as ~0 ^{14}C yr in the western subtropical Atlantic, has been proposed for HS1 [*Southon et al.*, 2012]. The spatial extent and the roles of local and regional influences on these low reservoir ages are still being investigated. Two recent studies suggest highly variable reservoir ages in the western subtropical Atlantic during the last deglaciation, with reservoir ages ranging from ~0 to 900 ^{14}C yr and large changes occurring over a couple hundred years [*Butzin et al.*, 2012; *Ramsey et al.*, 2012].

Iberian Margin reservoir ages have been studied using a series of cores from nearly identical latitude (38°N). *Waelbroeck et al.* [2001] reconstructed constant ~400 ^{14}C yr Iberian Margin reservoir ages during the last deglaciation. *Peck et al.* [2007] suggested near-modern Iberian Margin reservoir ages between 24 and 19 kyr BP with up to ~1000 ^{14}C yr reservoir ages between 17.3 and 16.4 kyr BP. *Skinner* [2008] proposed that Iberian Margin reservoir ages were ~430 ^{14}C yr older than Cariaco Basin reservoir ages before ~22 kyr BP. This could result from a decrease in Cariaco Basin reservoir ages, an increase in Iberian Margin reservoir ages, or both. *Ramsey et al.* [2012] reported Iberian Margin reservoir ages up to ~800 ^{14}C yr during the LGM and HS1.

Aside from these two specific regions, we must turn to modeling studies to get a sense of the potential variability in broader-scale low-latitude North Atlantic reservoir ages. Unfortunately, there is little agreement between model results on this subject. Glacial boundary conditions may have slightly increased [*Butzin et al.*, 2005] or decreased [*Franke et al.*, 2008] low-latitude reservoir ages, when present day Atlantic meridional overturning circulation (AMOC) is maintained. For a freshwater-induced AMOC reduction, low-latitude Atlantic reservoir ages may have decreased [*Delaygue et al.*, 2003; *Singarayer et al.*, 2008], increased

[*Franke et al.*, 2008], stayed the same [*Butzin et al.*, 2005], or decreased and then increased [*Ritz et al.*, 2008]. *Franke et al.* [2008] model the most variable low-latitude North Atlantic reservoir ages of any study; they suggest that low-latitude reservoir ages remain between ~300 and 500 ^{14}C yr except during the Laschamp and Mono Lake excursions when increased atmospheric Δ^{14}C causes reservoir ages of ~650 ^{14}C yr. Five of the low-latitude sites in our compilation come from the west African coast, and model results suggest that reservoir ages remain between ~250 and 550 ^{14}C yr during freshwater-induced AMOC reduction, despite enhanced upwelling in this area [*Ritz et al.*, 2008].

Based on the available evidence, it seems likely that averaged low-latitude North Atlantic reservoir ages remained within a couple hundred years of the modern ~400 ^{14}C yr average. Reservoir age changes of this magnitude are within the uncertainty of our low-latitude radiocarbon age model. At individual low-latitude sites, reservoir ages may have increased or decreased by up to ~400 ^{14}C yr.

7. Methods

HLNA reservoir age reconstruction

We compiled previously published planktonic ^{14}C dates, benthic δ^{18}O, IRD, and relative paleointensity (RPI) records for 33 deep (>2000 m) North Atlantic cores (Table S1). These cores all have benthic δ^{18}O records with an average resolution better than ~2000 yr over the studied interval and planktonic ^{14}C dates; fifteen cores also have IRD records; four Iberian Margin sites have RPI records. We made a new age model for each core based only on that core's ^{14}C dates using the Bayesian age modeling program Bchron [*Parnell et al.*, 2008] and the Marine09 calibration [*Reimer et al.*, 2009] with constant 405 ^{14}C yr reservoir ages. Bchron identifies outlying dates probabilistically and provides robust Monte Carlo error estimates for depths between dates. Due to computational limitations, certain cores with very many dates or significant outliers required multiple, overlapping (in the depth domain) Bchron runs which we then spliced together to create a single, continuous age model for each core. In these cases, boundaries between sections were chosen where the age versus depth relationship appeared smoothest and excellent agreement was achieved between overlapping sections. An additional difficulty is encountered when potentially outlying dates occur at the beginning or end of a sequence. In these cases, we deferred to the original authors to decide whether to include the very youngest or oldest dates for a particular core.

We aligned all the benthic $\delta^{18}O$ records to MD95-2042 [*Shackleton et al.*, 2000] using the automated alignment software Match [*Lisiecki and Lisiecki*, 2002]. Where available, IRD and RPI data also constrained the alignments. Multi-proxy alignments yield more robust core-to-core correlations by reducing the degrees of freedom for an alignment [*Channell et al.*, 2009]. For the alignments, benthic $\delta^{18}O$ and RPI records were normalized to have means = 0 and standard deviations = 1, while IRD records were scaled to have maximum values of 1. Tie points were added where needed. All benthic $\delta^{18}O$, IRD, and RPI alignments are shown in Figures S2-4.

We aligned the individual records on their own depth scales to MD95-2042 on the GICC05 age model [*Svensson et al.*, 2008]. The GICC05 age model merely acts as a placeholder here (rather than MD95-2042 depth), and our reservoir age determinations are not actually tied to the ice core chronology. We put MD95-2042 on the GICC05 age model by aligning planktonic $\delta^{18}O$ to NGRIP $\delta^{18}O$ using Match. Having MD95-2042 on an age model improves the alignments by removing its sedimentation rate changes. This is similar to the procedure used by *Lisiecki and Raymo* [2005], where their final alignments were performed using a "transitional stack" on a preliminary age model as the alignment target. *Channell et al.* [2009] also did their multi-proxy Match alignments using a target core on an age model rather than its depth scale.

Based on these alignments, we then used Bchron to generate age estimates at evenly spaced 500 yr intervals on the preliminary GICC05 age model for the low-latitude cores. For every 500 yr time step, we took the average of all available low-latitude Bchron-generated age estimates. This yields a preliminary low-latitude ^{14}C age model, versus GICC05 age (Figure S5).

Using the same alignments and this preliminary low-latitude ^{14}C age model, we next generated Bchron age estimates at evenly spaced 500 yr intervals for all cores on the low-latitude age model. Then we averaged these ages together to make separate high- and low-latitude ^{14}C age models. Simply comparing the two age models at this point would not provide true reservoir ages because the units are still in calendar years, not ^{14}C yr.

For every age step, we "uncalibrated" both the high- and low-latitude age models using Marine09, then compared these uncalibrated surface ocean ^{14}C ages to the contemporaneous atmospheric ^{14}C ages provided by IntCal09 [*Reimer et al.*, 2009]. This yields separate high- and low-latitude reservoir age estimates in units of ^{14}C yr. The empirically calculated low-latitude reservoir ages differ somewhat from the assumed constant value of 405 ^{14}C yr due to noise in the data and the fact that we fixed the age models at 0 kyr BP. Therefore, we subtracted the low- from the high-latitude reservoir ages then added 405 ^{14}C yr to get our final HLNA reservoir ages. This step corrects our reservoir age curve for the effects of anomalously old ages near the core-tops but has a negligible effect elsewhere.

Bchron-generated Monte Carlo samples were propagated through the entire procedure, providing robust 95% confidence intervals around our final HLNA reservoir age estimates.

The Vedde Ash occurs at 12.1 kyr BP (on our low-latitude ^{14}C age model) in five of the cores used in our compilation. This is consistent with the currently accepted age of the ash [*Rasmussen et al.*, 2006], confirming the reliability of our alignments and age models during the YD.

Planktonic foraminifera depth habitats

Radiocarbon dates from a variety of planktonic foraminifera species were used in our compilation, but the vast majority of dates come from *Neogloboquadrina pachyderma*, *Globigerina bulloides*, *Globorotalia inflata*, and *Globigerinoides sacculifer*. *G. bulloides* lives in the near-surface layer, between ~0-60 m water depth [*Ganssen and Kroon*, 2000], while *G. sacculifer* prefers mixed layer depths between ~20-40 m [*Farmer et al.*, 2007]. *G. inflata* occupies the bottom of the winter mixed layer, between ~100-300 m water depth [*Ganssen and Kroon*, 2000; *Salgueiro et al.*, 2010]. *N. pachyderma* calcifies in the lower mixed layer or pycnocline but reproduces below the pycnocline, giving apparent calcification depths of ~50-200 m [*Simstich et al.*, 2003; *Winsor et al.*, 2012]. The depth habitat of *N. pachyderma* (s) also depends on local salinity stratification, as this species does not tolerate low salinities [*Hillaire-Marcel and de Vernal*, 2008]. *N. pachyderma* (d) appears to occupy slightly shallower depths than *N. pachyderma* (s), but differences between these two could also be due to seasonality [*Benway et al.*, 2010].

Depth habitats are relevant for our study of reservoir ages because shallower-dwelling foraminfera might be expected to better record surface conditions, while deeper-dwelling species might be more influenced by subsurface-to-intermediate depth water masses. In practice, this potential complication is difficult to assess with respect to planktonic radiocarbon dates because few cores contain levels that have been dated using multiple species independently. A third of the records used in our compilation have radiocarbon dates based on a single species for the entire record (although different species are used between these cores). Most workers date monospecific samples from local abundance maxima in the core to minimize the effects of bioturbation [*Bard et al.*, 1987a], although two to three species may be dated along the length of the core (one species during warm intervals and another during cold intervals, for example). Finally, a few records in our compilation include dates from mixed assemblages of planktonic foraminifera. Usually, when independent dates are taken from different planktonic species at the same level in a core, the dates agree within their uncertainties [e.g., *Skinner and Shackleton*, 2004]. Rare discordances between dates from different species have been attributed to differential dissolution and fragmentation of fragile versus robust shells and sediment reworking, rather than differences in depth habitat [*Broecker et al.*, 2006; *Barker et al.*, 2007].

Depth habitats are of particular interest regarding our interpretation of the HLNA reservoir age decrease around 16 kyr BP, where our explanation calls on freshwater-induced surface stratification limiting mixing from below and allowing surface equilibration with the atmosphere. Many of the foraminifera species that constrain our age models are not true surface dwellers, and *N. pachyderma* (s) would have likely migrated deeper in response to surface freshening [*Hillaire-Marcel and de Vernal*, 2008].The fact that our average HLNA reservoir age at 16 kyr BP (~700 ^{14}C yr) is somewhat larger than the modern regional average (~400-500 ^{14}C yr), despite model results suggesting that freshwater-induced stratification would lead to slightly smaller than modern reservoir ages [*Ritz et al.*, 2008], might be partly due to subsurface dwelling foraminifera recording the influence of deeper water masses. This highlights the importance of models presenting reservoir age results for actual foraminifera living depths, rather than just the actual surface of the ocean, to allow for better model-data comparisons. Because our composite age models and HLNA reservoir age reconstruction include dates from many different locations and species, they are probably best interpreted as representing the average age of the upper couple hundred meters of the water column and they should be less sensitive than an individual record to the living preferences of any particular species.

IRD stack

Our IRD stacking methods basically follow those used by *Lisiecki and Raymo* [2005] for the construction of their benthic $\delta^{18}O$ stack. We used our alignments to transfer scaled IRD values from their original depths, to GICC05 age, and finally to low-latitude ^{14}C age. The IRD stack was created with 500-yr resolution on the low-latitude ^{14}C age model. Each stacked value represents the average of all available scaled IRD values within ±250 yr. This technique weights high-resolution records more than low-resolution records and avoids the use of any interpolated IRD values.

There are a number of ways to quantify the IRD content of a sediment core, based on either absolute counts of coarse lithic fragments or percentages of total sediment, and different authors sometimes use different size fractions [*Hemming*, 2004]. Because of this, we stacked the scaled versions of IRD records that also constrained our alignments. Our IRD stack is thus presented in arbitrary units. This IRD stack is well suited for evaluating the timing of IRD, but our scaling process may distort the relative magnitude of the IRD peaks because not all IRD records extend over the entire studied interval.

Some of the effects of combining different types of IRD records over such a broad region can be seen in Figure S6, where we show separate IRD stacks for percent (%) vs. absolute count (#/g) IRD records and east vs. west North Atlantic IRD records. Here, “west” refers to core locations on or west of the Mid-Atlantic Ridge; “east” refers to core locations east of the Mid-Atlantic Ridge. The IRD peak during HS3 is much more pronounced in the % IRD stack compared to the #/g IRD stack, consistent with Heinrich Event 3 being affected by an interval of low foraminifera abundance (as mentioned in Section 4 of the auxiliary materials). The east IRD stack has a single peak during HS1 at 16 kyr BP, consistent with the established timing of a major European-sourced IRD event (discussed in the main text). In contrast, the west IRD stack contains two peaks during HS1: the earlier peak at 17 kyr BP likely corresponds to the Laurentide-sourced Heinrich Event 1, while the later peak at 16 kyr BP correlates with the European-sourced peak in the east IRD stack. These features confirm the quality of our alignments over HS1. The early HS1 IRD peak (Heinrich Event 1; ~17 kyr BP) appears stronger in the % IRD stack compared to the #/g IRD stack. This could reflect the higher resolution of the two western % IRD records compared to the two eastern % IRD records, the influence of a low foraminifera abundance event, and/or the generally noisier nature of the % IRD stack as it only contains four records.

8. Alignment perturbations

Assessing the uncertainty associated with the alignment of paleoclimate records is an important but formidable task, and formal alignment uncertainty calculations are beyond the scope of this work. In general, we expect benthic $\delta^{18}O$ changes to be synchronous within a few hundred years in the deep North Atlantic (as discussed in Section 3 of the auxiliary materials). Small diachroneities probably account for some of the scatter in radiocarbon ages shown in Figure S5, and this scatter is taken into account in our age model and reservoir age uncertainty calculations. Our averaging technique minimizes the effects of small diachroneities between individual benthic $\delta^{18}O$ records, and further alignment constraints from IRD records, Iberian Margin RPI records, and the Vedde Ash add robustness to our results. Nonetheless, despite our best intentions and careful attention to detail, it is possible that we have misaligned a small number of records, so here we investigate the effects of misalignment on our reservoir age results.

To investigate the effects of one or two alignments being off by up to 2 kyr, we artificially adjusted some of our alignments by adding or subtracting 2 kyr at 17 kyr BP and tapering linearly to no adjustment at 12 and 22 kyr BP (on the preliminary GICC05 age model). We centered the perturbations at 17 kyr BP to focus our investigation on HS1 reservoir age changes. Proportionately smaller perturbations to more records should provide similar results.

In the low latitudes, cores EW9209-2 and EW9209-3 have distinct light benthic $\delta^{18}O$ anomalies during HS1 that are not present in other records. These records also have fairly low sedimentation rates (~5 cm/kyr average), are dated with low sampling resolution, and lack other types of paleoclimate records (except benthic $\delta^{13}C$) to corroborate their alignments. So, we tested the effects of shifting both these records to older aligned ages and both these records to younger aligned ages (following the procedure outlined in the previous paragraph).

In the high latitudes, we investigated the effects of individual alignments on the large early HS1 reservoir ages and the small late HS1 reservoir ages. SU90-11 has the largest early HS1 reservoir ages, so we shifted this alignment to older aligned ages to decrease the average early HS1 reservoir age. GIK17049 has the smallest late HS1 reservoir ages, so we shifted this alignment to younger aligned ages to increase the average late HS1 reservoir age.

These four experiments where we shifted one or two alignments by up to 2 kyr resulted in only very small (up to ~200 ^{14}C yr) changes in the average HLNA reservoir age curve (Figure S7). The four reservoir age curves that include perturbed alignments all lie within the reported uncertainty of our actual reservoir age curve, confirming that our average HLNA reservoir age history is robust to alignment errors of up to 2 kyr in one or two cores.

9. Sedimentation rates

The bioturbation of ocean sediments has been recognized as an important source of uncertainty in past HLNA reservoir age reconstructions since the first estimates were published by *Bard et al.* [1994]. Calculations by *Bard et al.* [1994] suggest possible age biases of ~500 ^{14}C yr for a mixing depth of 10 cm and sedimentation rate of 8 cm/kyr. Average sedimentation rates range from about 4 to 65 cm/kyr for the cores used in this study, based on our low-latitude ^{14}C age model (Figure S8).

In particular, we wish to address the possibility that our relatively small late HS1 reservoir ages (which disagree with some previous studies, discussed further in Section 12 of the auxiliary materials) may have been influenced by downward mixing of Bølling-Allerød aged sediments at low sedimentation rate core locations. To do this, we recalculated average HLNA reservoir ages after removing records that have sedimentation rates <5 cm/kyr at any time between 18-13 kyr BP on our low-latitude ^{14}C age model. This criterion removed cores EW9209-1, EW9209-2, EW9209-3, GIK13289, ODP658C, SU90-03, SU90-08, SU90-11, GIK17045, GIK23415, GIK17049, GIK17051, and V29-202. The reservoir age curve calculated from only high sedimentation rate cores is shown in Figure S9. The general pattern of large early HS1 reservoir ages and small late HS1 reservoir ages remains, with the transition between about 16.5 and 16.0 kyr BP, although the major decrease in reservoir ages over the early/late HS1 boundary occurs 500 yr later in the high sedimentation rate reservoir age curve. The high sedimentation rate reservoir age curve suggests smaller BA reservoir ages and a more rapid transition to large YD reservoir ages. All these changes are within the reported uncertainty of the composite reservoir age curve. Small reservoir ages during late HS1 and the rapid decrease in reservoir ages around 16 kyr BP do not appear to be artifacts of bioturbation, nor are these features affected by our use of low sedimentation rate cores.

10. New ^{14}C calibration curves

Three studies [*Hoffmann et al.*, 2010; *Ramsey et al.*, 2012; *Southon et al.*, 2012] have provided significant additions to the available radiocarbon calibration data since the publication of IntCal09 and Marine09 [*Reimer et al.*, 2009]. Potential updates to IntCal09 and Marine09 during HS1 are of particular interest.

IntCal04 [*Reimer et al.*, 2004] and Marine04 [*Hughen et al.*, 2004] included ^{14}C data from the western subtropical Atlantic with the assumption of constant ~400 ^{14}C yr reservoir ages. Because consensus has emerged that reservoir ages in this region decreased during the early YD, IntCal09 and Marine09 did not include western subtropical Atlantic data from this interval [*Reimer et al.*, 2009]. Recent work from Hulu Cave [*Southon et al.*, 2012] and Lake Suigetsu [*Ramsey et al.*, 2012] supports a similar decrease in western subtropical Atlantic reservoir ages across the early/late HS1 boundary (Figure S10).

There are two conceivable ways this change in the calibration curve could affect our results during HS1. First, our low latitude ^{14}C age model would shift to older ages by up to ~400 yr between ~17 and 15.5 kyr BP. As the resolutions of our IRD stack and HLNA reservoir age reconstruction are 500 yr, we consider this shift to be negligible. Second, we must consider what effect this update would have on the HLNA reservoir ages. We argue that our method is insensitive to subtle changes in the calibration curve because we take the difference between uncalibrated high- and low-latitude ^{14}C ages (plus 405 ^{14}C yr) as our reservoir ages.

11. Spatial variability in HLNA reservoir ages

We produce a single averaged reservoir age history for the HLNA because reservoir ages calculated for individual sites have much larger uncertainties than a composite record. However, previous workers have noted the possibility of zonal and meridional gradients in HLNA reservoir ages when the AMOC is reduced [*Bard*, 1988; *Ritz et al.*, 2008; *Rashid et al.*, 2012]. Such gradients could bias our average HLNA reservoir ages and limit the applicability of our results to additional sites.

In general, we would expect HLNA reservoir ages to increase with latitude when the AMOC is reduced, similar to the modern high-latitude Southern Ocean and North Pacific [*Bard*, 1988]. However, no significant meridional trend is present either in previous work [*Waelbroeck et al.*, 2001] or in our study (Figure S11) during HS1 and the YD. *Rashid et al.* [2012] suggest larger reservoir ages in the eastern compared to western Atlantic at 34°N during HS1. In contrast, model results suggest larger reservoir ages in the western compared to eastern North Atlantic during AMOC reduction [*Ritz et al.*, 2008]. *Cao et al.* [2007] compare estimates from several studies and conclude that no significant zonal gradient was present in YD HLNA reservoir ages.

Thus, it is not immediately clear what kind of spatial variability in HLNA reservoir ages we might expect with reduced AMOC. As we suggest in this study, AMOC reduction might increase or decrease HLNA reservoir ages, depending on location, magnitude, and duration of freshwater input. These same melting factors could influence the AMOC and thus spatial variability in reservoir ages differently. For example, *Bard et al.* [1994] argued that weakening of the Gulf Stream and lower North Atlantic Deep Water (NADW) formation would increase HLNA reservoir ages, while weakening the northward transport of thermocline waters and upper NADW formation in the Labrador Sea would have no effect on HLNA reservoir ages.

Figure S11 and Table S2 provide reservoir age estimates for individual cores used in this study for select time slices. There are no obvious trends with either latitude or longitude, nor are there any apparent differences between marginal and open ocean sites. However, the western HLNA is underrepresented in our compilation, so zonal gradients in past reservoir ages may become apparent with the addition of more data from this region in the future. Again, we emphasize that reservoir ages calculated for individual sites have much larger uncertainties than our composite HLNA reservoir ages.

12. Comparison with other late HS1 reservoir age estimates

A fairly comprehensive comparison of our HLNA reservoir ages with estimates from previous studies is provided in Figure S12. Each of the various time intervals of interest are discussed in the main text. Here, we elaborate on the differences between our relatively small late HS1 reservoir ages and the generally larger estimates provided by four separate studies.

Waelbroeck et al. (2001). The disagreement between our late HS1 HLNA reservoir age results and those of *Waelbroeck et al.* [2001] (hereafter, W01) are particularly surprising. The three marine cores used by W01 are all included in our compilation. W01 compared the ^{14}C ages of two rapid warming events (HS1/BA and YD/Holocene transitions) in marine sea surface temperature (SST) records with the ages given by Greenland ice core chronologies to develop their reservoir age estimates. W01 did not directly use benthic $\delta^{18}O$ alignments to reconstruct reservoir ages (as we did), but they did note improved benthic $\delta^{18}O$ alignments after applying their increased reservoir ages for high-latitude cores.

We reconstructed W01's reservoir ages to investigate whether updates to the Greenland ice core age model or radiocarbon calibration curve, or using Bchron versus polynomial interpolation, could explain the disagreement (Table S3). The midpoint of the HS1/BA transition in Greenland is 100 yr older on the new ice core chronology, which would slightly decrease the calculated reservoir ages. On our chronologies (using Marine09, Bchron, and constant 405 ^{14}C yr reservoir ages), the midpoint of the HS1/BA warming occurs 200 yr later in NA87-22 and 300 yr earlier in CH69-K9, compared to W01's results. The age shift of NA87-22 is within W01's reported uncertainty, while that of CH69-K9 is outside W01's reported uncertainty. However, the age uncertainties we calculated for these cores (95% confidence intervals) are larger than those of W01, suggesting that W01 may have underestimated the age uncertainties for their high-latitude sites. As a result of the Greenland ice core age model update, small shifts in re-calculated age models for these cores, and the use of different radiocarbon calibration curves, we calculate reservoir ages at the HS1/BA transition that are over 700 ^{14}C yr smaller for NA87-22 and about 100 ^{14}C yr smaller for CH69-K9, compared to W01. After these adjustments, there is considerable overlap between the lower bounds of reservoir ages estimated for these cores (~770 ^{14}C yr) and the upper bound of our estimate of mean HLNA reservoir age at 15 ka (970 ^{14}C yr). Additionally, our calculated reservoir ages for NA87-22 and ODP 980 (from a nearly identical location and using radiocarbon dates from *Benway et al.* [2010]) agree within about 100 ^{14}C yr during late HS1 and the BA (Figure S11 and Table S2).

Björck et al. (2003). Using four sites, *Björck et al.* [2003] (hereafter, B03) reconstruct an average of ~1000 ^{14}C yr HLNA reservoir ages from 15 kyr BP through the end of the YD, with significant scatter in their individual estimates. All but one of B03's late HS1 reservoir age estimates are within error of our reconstructed values. B03's largest late HS1 reservoir age estimate (~1500 ^{14}C yr at 15 kyr BP) comes from their highest latitude site (63°N). This site is located poleward of our northernmost site, and may record larger reservoir ages than our averaged HLNA estimates. B03's reliance on a now-outdated Greenland ice core chronology and their extrapolation of estimated terrestrial ^{14}C ages may also contribute to the discrepancy. Additionally, the oldest reservoir age reported by B03 occurs at the oldest ^{14}C date for one of their cores, and it is difficult to identify outlying ^{14}C dates at the beginning or end of a sequence of dates.

Peck et al. (2007). *Peck et al.* [2007] (hereafter P07) suggest a reservoir age of ~2000 yr at 15.1 kyr BP for core MD01-2461 in the northeast Atlantic. P07's reservoir age estimates are reported in calendar years, but converting to radiocarbon years still yields an estimate of ~1700 ^{14}C yr, much larger than our late HS1 average HLNA reservoir age estimates of around 500-700 ^{14}C yr. Core MD01-2461 is not included in our study because it is from intermediate water depths, but two cores in our compilation also show reservoir ages of ~1500-1700 ^{14}C yr during late HS1 (Figure S11 and Table S2). Individual estimates of reservoir ages at any particular time can display significant scatter about the mean but do not show any particular spatial pattern.

Thornalley et al. (2011). *Thornalley et al.* [2011b, 2011c] (hereafter T11) report late HS1 reservoir ages up to 2000 ^{14}C yr for four cores located south of Iceland between 61 and 63°N. These core locations are near modern deep water convection and overflow sites. Although the age models of T11's cores are well constrained by tephra correlations, unique oceanographic conditions at this locality mean that these reservoir age estimates are probably not representative of average HLNA conditions: "Mixing with underlying [southern-sourced waters] may have been greater on the South Iceland Rise than that in more open ocean sites because of coastal upwelling and turbulent mixing caused by interaction with seafloor topography" [*Thornalley et al.*, 2011a]. Thus, radiocarbon-depleted waters from the Southern Hemisphere or Nordic Seas may have contributed to these old reservoir ages [*Thornalley et al.*, 2011b]. Several other cores used in our study were taken from areas with rough bathymetry around continental margins where similar arguments might apply, but we observe no obvious systematic differences between past reservoir ages at marginal versus open ocean sites (Figure S11).

13. Potential mechanisms for changes in HLNA reservoir ages

In the main text, we called on AMOC reductions and shifts in the polar front to explain HLNA reservoir age changes at the beginning (~19 kyr B.P.) and middle (~16 kyr B.P.) of HS1. The magnitudes of the reservoir age changes we observe appear to require such mechanisms. However, many other factors can cause small reservoir age changes, and these may have also contributed to the changes we observe. Here, we provide an outline of the potential effects on HLNA reservoir ages for different mechanisms. In some cases, these effects might be linked through (linear or nonlinear) feedbacks.

<u>AMOC reduction and southward shift of the polar front.</u> Reduced northward advection of tropical surface waters and an associated southward shift in the polar front are implicated as a primary cause for increased HLNA reservoir ages during HS1 and the YD by virtually all studies that have made such observations [*Bard et al.*, 1994; *Waelbroeck et al.*, 2001; *Bondevik et al.*, 2006; *Cao et al.*, 2007; *Knutz et al.*, 2007; *Austin et al.*, 2011; *Hall et al.*, 2011; *Thornalley et al.*, 2011b]. This mechanism implies a meridional contraction of the AMOC cell and at least a partial reduction in North Atlantic Deep Water (NADW) formation because these warm, salty tropical waters feed modern NADW. Even with increased reservoir ages and the implied AMOC reduction, deep waters may still be formed south of the polar front [*Austin et al.*, 2011], weak convection might continue north of the polar front [*Waelbroeck et al.*, 2001], and upper deep waters fed by high-latitude upwelling of thermocline and intermediate waters (akin to modern Labrador Sea processes) could potentially form [*Bard et al.*, 1994]. Although data studies agree on the importance of AMOC reduction and a southward shift of the polar front for causing increased HLNA reservoir ages, models have not been able to demonstrate this effect, especially

for large >1000 ^{14}C yr reservoir ages that we and others observe during HS1. (One simple box model [*Bard*, 1988] is an exception.) Most modeling studies addressing reservoir ages have focused on the YD and used present day boundary conditions [*Stocker and Wright*, 1996; *Delaygue et al.*, 2003; *Ritz et al.*, 2008; *Singarayer et al.*, 2008]. These studies were often trying to model features of the Cariaco Basin atmospheric $\Delta^{14}C$ record, which probably overestimated peaks during HS1 and the early YD, as discussed earlier. Even when glacial boundary conditions are used [*Butzin et al.*, 2005], the duration of HS1 melting may have been underestimated. In addition, the specific location of freshwater input probably has ramifications for the impacts that melting has on the AMOC [*Roche et al.*, 2010]. Of course, data reconstructions have their limitations as well, and different HLNA reservoir age estimates are not in perfect agreement during HS1 and the YD. Our estimates suggest large reservoir age changes, but the lower limit of our early HS1 95% confidence intervals ranges from 440 to 800 ^{14}C yr, allowing for the possibility of much smaller HLNA reservoir age variability. We suggest that future modeling efforts into HS1 HLNA reservoir age variability include realistic ice sheets (which influence the polar front position), realistic melting history (volume and location), and realistic sea surface temperature evolution.

<u>Sea ice.</u> The presence of sea ice increases reservoir ages by suppressing air-sea gas exchange [*Bard*, 1988]. Reduced AMOC, a southward shift in the polar front, and bipolar seesaw cooling in the HLNA are all clearly compatible with increasing sea ice as well. Sea ice is regularly invoked as a contributor to increased HLNA reservoir ages [*Bard et al.*, 1994; *Waelbroeck et al.*, 2001; *Bondevik et al.*, 2006; *Knutz et al.*, 2007; *Austin et al.*, 2011; *Hall et al.*, 2011; *Thornalley et al.*, 2011b]. Models generally agree that the presence of sea ice can increase reservoir ages by up to ~200-300 ^{14}C yr [*Bard et al.*, 1994; *Stocker and Wright*, 1996;

Singarayer et al., 2008]. Even if sea ice extended all the way to ~40°N for a full 12 months per year during early HS1 (which is unlikely), this would be a minor effect in comparison to the observed >1000 ^{14}C yr HLNA reservoir ages.

Surface-to-deep ocean mixing. The introduction of an especially ^{14}C-depleted intermediate-to-deep water mass or enhanced upwelling could potentially increase surface reservoir ages. If radiocarbon-deficient Antarctic Intermediate Water (AAIW) extended farther northward during the YD and HS1, this could contribute to increased HLNA reservoir ages [*Cao et al.*, 2007; *Thornalley et al.*, 2011a, 2011b]. However, the extent of AAIW in the Atlantic during the YD and HS1 is still being debated [*Pahnke et al.*, 2008; *Xie et al.*, 2012]. The Nordic Seas are another possibility for a depleted intermediate-to-deep water mass [*Thornalley et al.*, 2011b]. The size of surface reservoir age changes that would be produced by introducing a depleted intermediate-to-deep water mass is not well constrained and would depend on the magnitude of depletion and degree of upwelling. Models show that decreasing the ventilation of the deep ocean has a major effect on the radiocarbon content within the deep North Atlantic (i.e., the benthic-planktonic ^{14}C age difference), but very little effect on surface reservoir ages [*Bard*, 1988; *Stocker and Wright*, 1996; *Butzin et al.*, 2005]. The vertical diffusivity parameter in models affects both ^{14}C mixing and convection, but adjustments to this parameter probably have a negligible effect on both surface and atmospheric $\Delta^{14}C$ [*Bard*, 1988; *Delaygue et al.*, 2003].

^{14}C production rate. Changes in the production rate of ^{14}C in the atmosphere could also affect reservoir ages. An increase (decrease) in ^{14}C production causes a transient increase (decrease) in reservoir ages because of the time delay required for the surface ocean to return to steady-state [*Bard*, 1988; *Franke et al.*, 2008]. *Björck et al.* [2003] call upon such a mechanism to explain minor oscillations in their deglacial reservoir age reconstruction. However, these authors allow that some of their data are not suitable for determining reservoir ages. Their large reservoir ages during late HS1 and the BA disagree with other studies (including our own), and the oscillations they attribute to production changes are not statistically significant. Production rate effects on reservoir ages would be short-lived, global, and relatively small (except maybe in the Southern Ocean) [*Bard*, 1988; *Franke et al.*, 2008]. It is noteworthy that we do not observe an increase in HLNA reservoir ages during either the Laschamp (~41 kyr BP) or Mono Lake (~34 kyr BP) excursions. Production rates of cosmogenic isotopes (such as ^{14}C) can be independently reconstructed by global paleointensity records [*Laj et al.*, 2004] and ice core ^{10}Be [*Muscheler et al.*, 2004]. Deconvolution of the atmospheric $\Delta^{14}C$ record shows that deglacial changes in atmospheric $\Delta^{14}C$ were caused by ocean circulation changes and increasing atmospheric CO_2 [*Lal and Charles*, 2007]. Many studies agree that ocean $\Delta^{14}C$ controlled atmospheric $\Delta^{14}C$ during the deglaciation, not the other way around [*Bondevik et al.*, 2006; *Singarayer et al.*, 2008; *Austin et al.*, 2011; *Southon et al.*, 2012].

Wind stress (speed). An increase (decrease) in wind stress enhances (reduces) air-sea gas exchange and decreases (increases) surface ocean reservoir ages. Realistic changes in wind stress for LGM and deglacial conditions only result in very small (~100 ^{14}C yr maximum) reservoir age changes [*Bard*, 1988; *Bard et al.*, 1994; *Delaygue et al.*, 2003; *Butzin et al.*, 2005].

Addition of ^{14}C-depleted meltwater. Flooding of the North Atlantic with ^{14}C-depleted meltwater might increase reservoir ages in this region [*Knutz et al.*, 2007; *Hall et al.*, 2011], but there are no available estimates of the magnitude of this effect. Additionally, meltwater input might lead to stratification and rapid equilibration with the atmosphere, such as we propose happened during late HS1. This effect appears in several model results [*Stocker and Wright*, 1996; *Delaygue et al.*, 2003; *Ritz et al.*, 2008; *Singarayer et al.*, 2008].

Sea surface temperature. "A decrease in temperature affects the solubility of CO_2 (increases), the piston velocity (decreases) and the kinetic isotopic fractionation factors (increases). However, the overall effect is rather small since the different components vary in opposite directions." [*Bard et al.*, 1994]

Atmospheric CO_2 concentration. Decreasing atmospheric CO_2 by ~100 ppmv would cause a ~100-200 ^{14}C yr increase in reservoir ages [*Bard*, 1988; *Bard et al.*, 1994]. This effect would be globally distributed. *Butzin et al.* [2005] model a ~200 ^{14}C yr reservoir age increase (compared to modern) for most areas when they use glacial sea surface temperatures, atmospheric $\Delta^{14}C$, and CO_2, consistent with these earlier results.

Ocean surface area. The surface area of the glacial ocean was reduced relative to modern, which might cause global reservoir age increases up to ~100 ^{14}C yr [*Bard*, 1988].

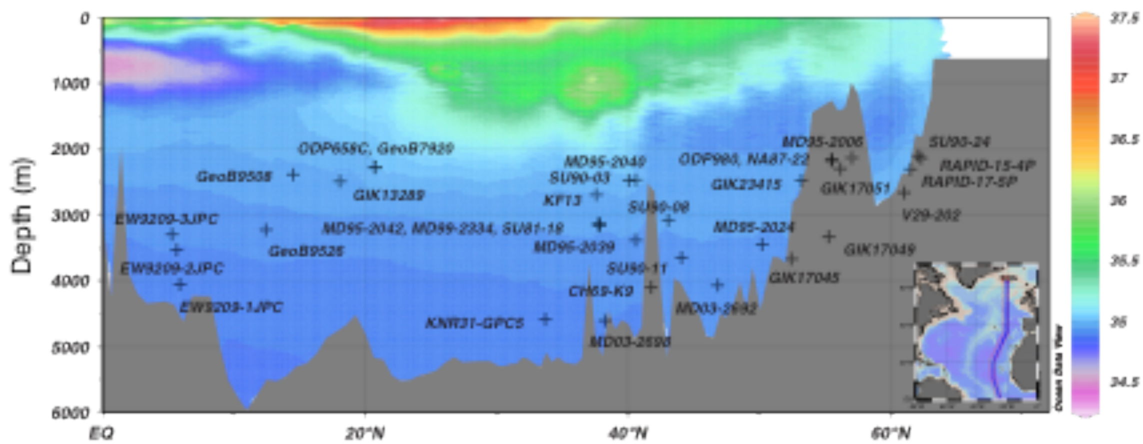

Figure S1: Zonally compressed latitude versus depth profile showing the locations of core sites used in this study. Colors indicate salinity, based on data from the WOCE A16 transect (cruise track shown in the inset in the bottom right).

Figure S2 (next page): Benthic $\delta^{18}O$ alignments for (a) low-latitude and (b) high-latitude sites. All records are on our low-latitude ^{14}C age model, ordered by increasing latitude from top to bottom. Triangles below each record indicate the position of radiocarbon dates for that record. A small number of dates that contributed to the age models but were taken from depths slightly outside the range of the benthic $\delta^{18}O$ records are not shown. Records were normalized for the alignments, so no y-axis is given. Gray vertical bars indicate the Younger Dryas (YD) and Heinrich stadials (HS) 2-4. The light blue and yellow vertical bars indicate early and late HS1, respectively.

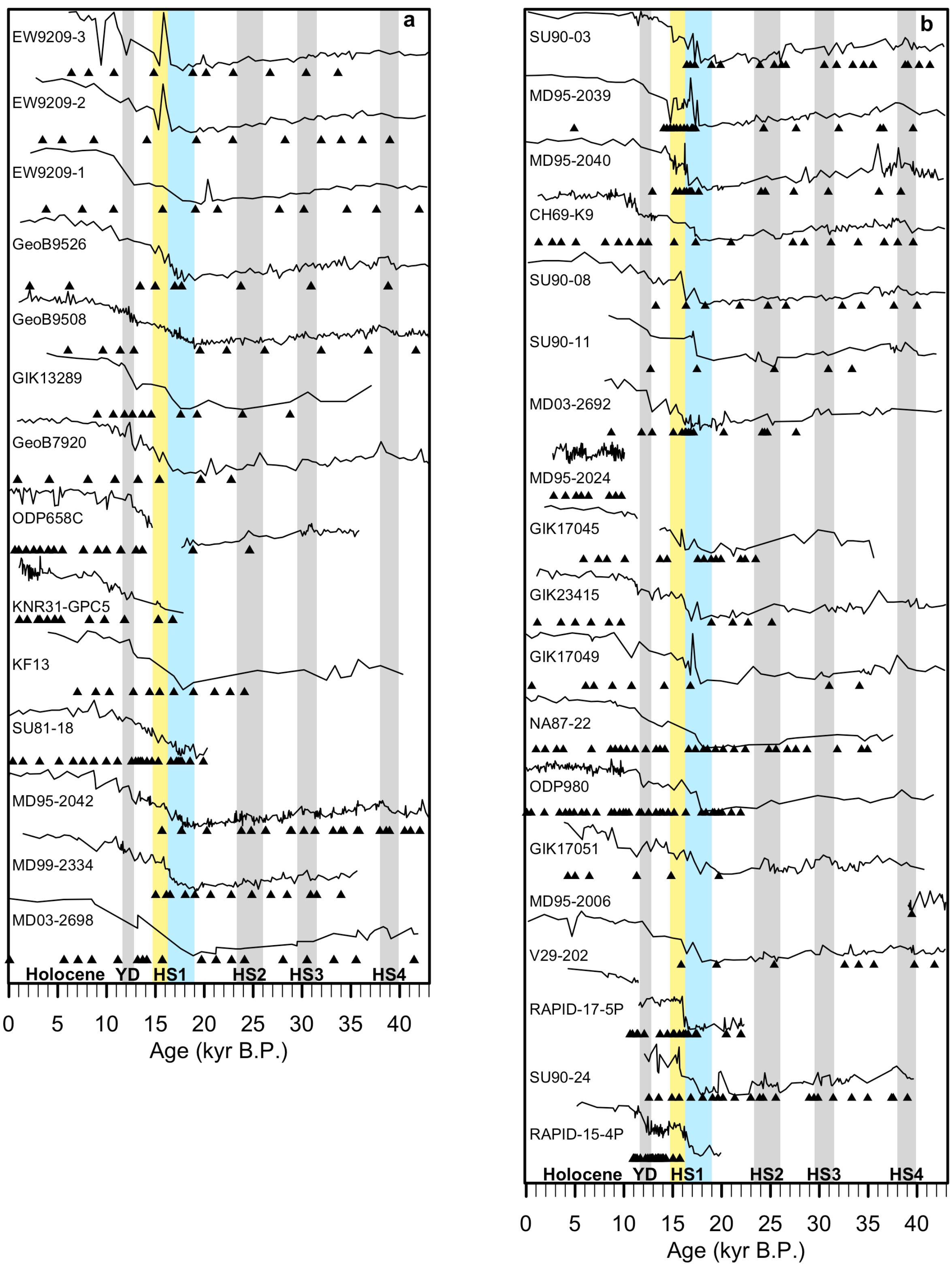
a
EW9209-3
EW9209-2
EW9209-1
GeoB9526
GeoB9508
GIK13289
GeoB7920
ODP658C
KNR31-GPC5
KF13
SU81-18
MD95-2042
MD99-2334
MD03-2698
Holocene YD HS1 HS2 HS3 HS4
0 5 10 15 20 25 30 35 40
Age (kyr B.P.)
b
SU90-03
MD95-2039
MD95-2040
CH69-K9
SU90-08
SU90-11
MD03-2692
MD95-2024
GIK17045
GIK23415
GIK17049
NA87-22
ODP980
GIK17051
MD95-2006
V29-202
RAPID-17-5P
SU90-24
RAPID-15-4P
Holocene YD HS1 HS2 HS3 HS4
0 5 10 15 20 25 30 35 40
Age (kyr B.P.)

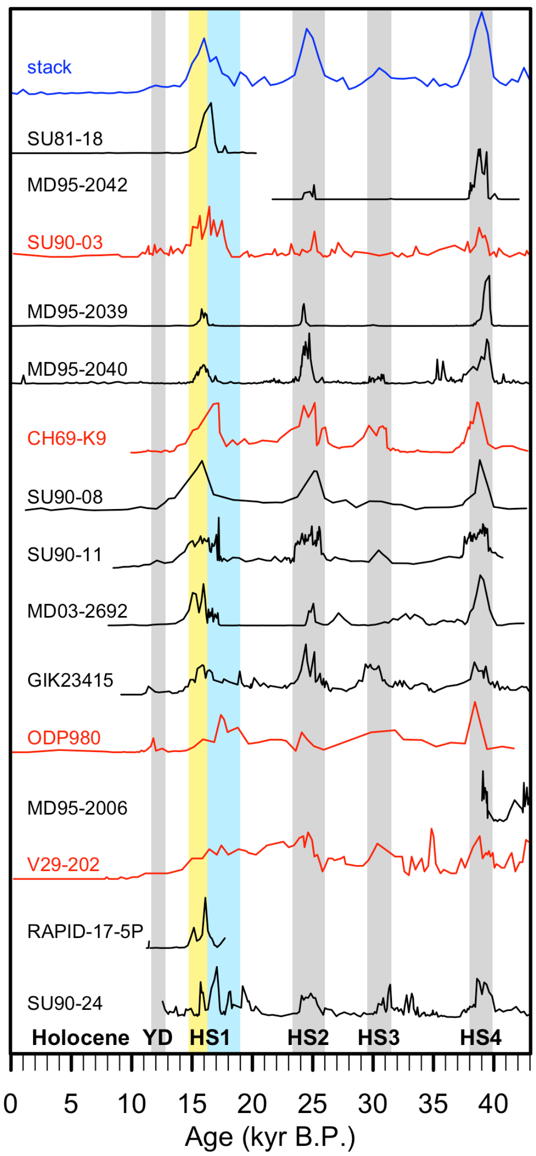

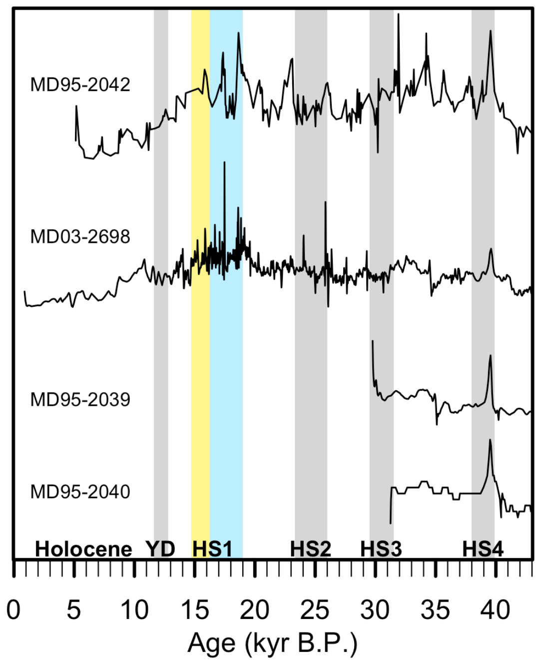

Figure S4 (above): Relative paleointensity (RPI) alignments. The four Iberian Margin RPI records are on our low-latitude ^{14}C age model. Records were normalized for the alignments, so no y-axis is given. Vertical bars as in Fig. S2.

Figure S3 (left): Ice-rafted debris (IRD) alignments. The individual IRD records (black and red) and IRD stack (blue) are on our low-latitude ^{14}C age model. Records in black reported IRD as absolute counts of coarse lithic fragments; records in red reported IRD as percentages of total sediment. All records were scaled for the alignments, so no y-axis is given. Vertical bars as in Fig. S2.

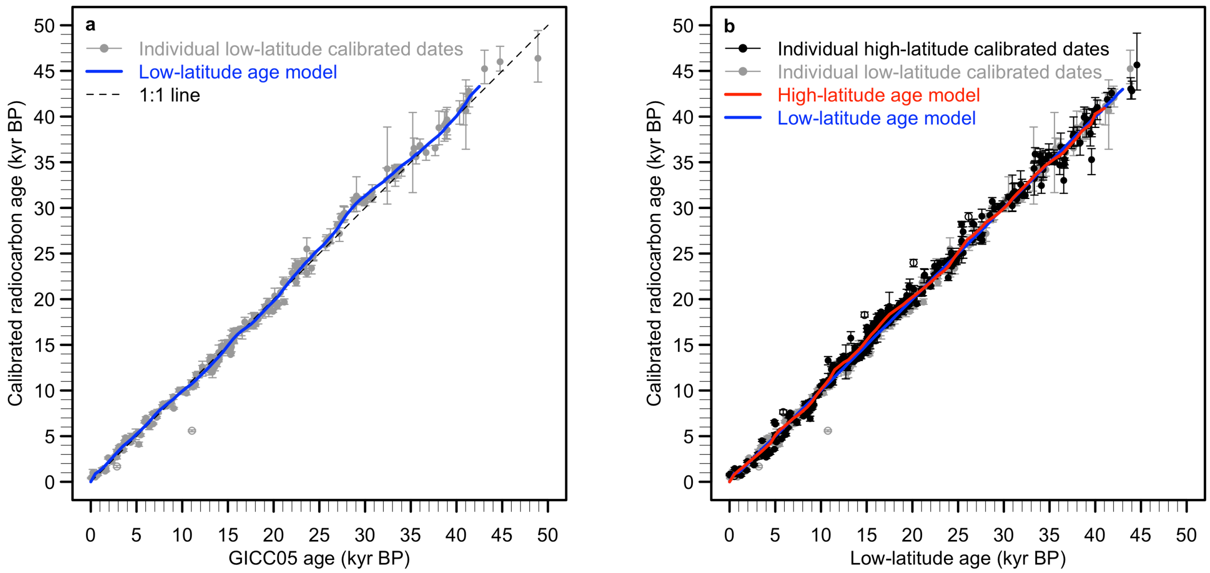

Figure S5: Individual radiocarbon dates and age model comparisons. (a) Low-latitude age model and dates versus GICC05 age. The only significant departure of the low-latitude age model from the 1:1 line is from ~23-35 kyr BP, similar to observations made by *Skinner* [2008]. (b) High- and low-latitude age models and dates versus the low-latitude ^{14}C age model. For (a and b), error bars on individual dates show 95% confidence intervals and open symbols indicate Bchron-identified outliers.

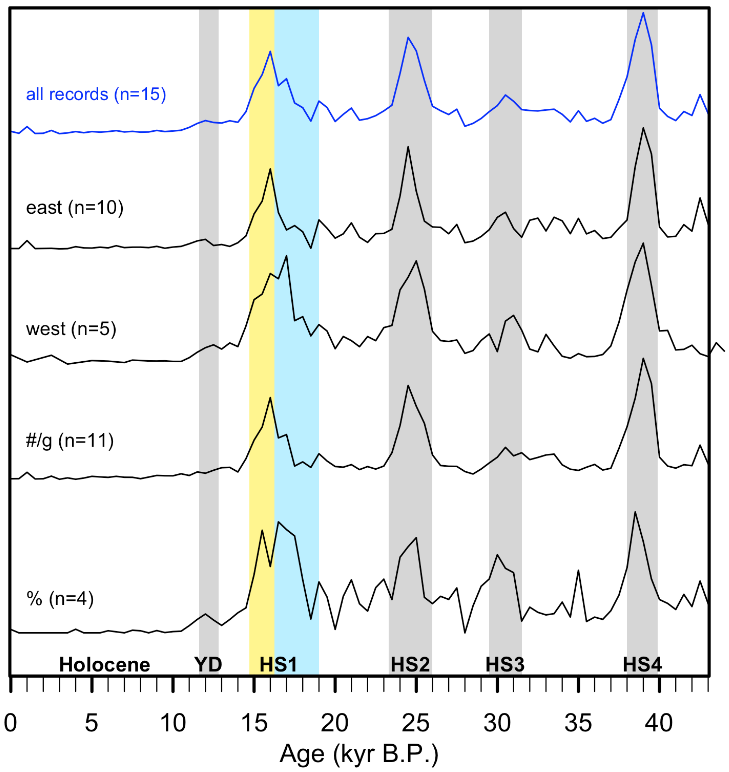

Figure S6: Different versions of the IRD stack, each with 500-yr resolution on our low-latitude ^{14}C age model. The IRD stack at the top (in blue) includes all available IRD records and is also shown in Figures 2, 3, and S3. The east IRD stack only includes records taken from east of the Mid-Atlantic Ridge. The west IRD stack includes records taken from west of and along the Mid-Atlantic Ridge. The "#/g" IRD stack only includes records reported as absolute counts of coarse lithic fragments. The "%" IRD stack only includes records reported as percentages of total sediment. The number of records included in each stack is indicated in parentheses in the figure. Vertical bars as in Fig. S2.

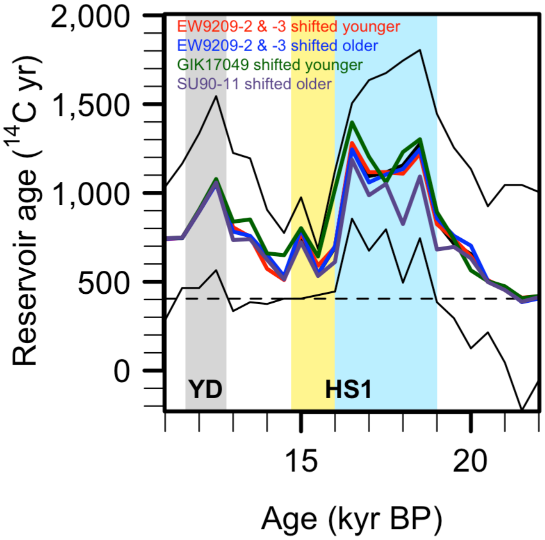

Figure S7: Alignment perturbation effects on average reservoir ages. The four colored lines show different versions of our average HLNA reservoir age history with one or two alignments artificially shifted by up to 2 kyr. The bold black line is our actual HLNA reservoir age history, thin black lines are the 95% confidence limits, and the dashed line indicates the modern global average reservoir age of 405 ^{14}C yr. Vertical bars as in Fig. S2.

Figure S8 (next page): Sedimentation rates for (a) low-latitude and (b) high-latitude cores used in this study based on our low-latitude ^{14}C age model, in units of cm/kyr. The extreme and unrealistic variability of MD95-2042's sedimentation rate results from our alignment of that core's planktonic δ^{18}O to NGRIP δ^{18}O. Vertical bars as in Fig. S2.

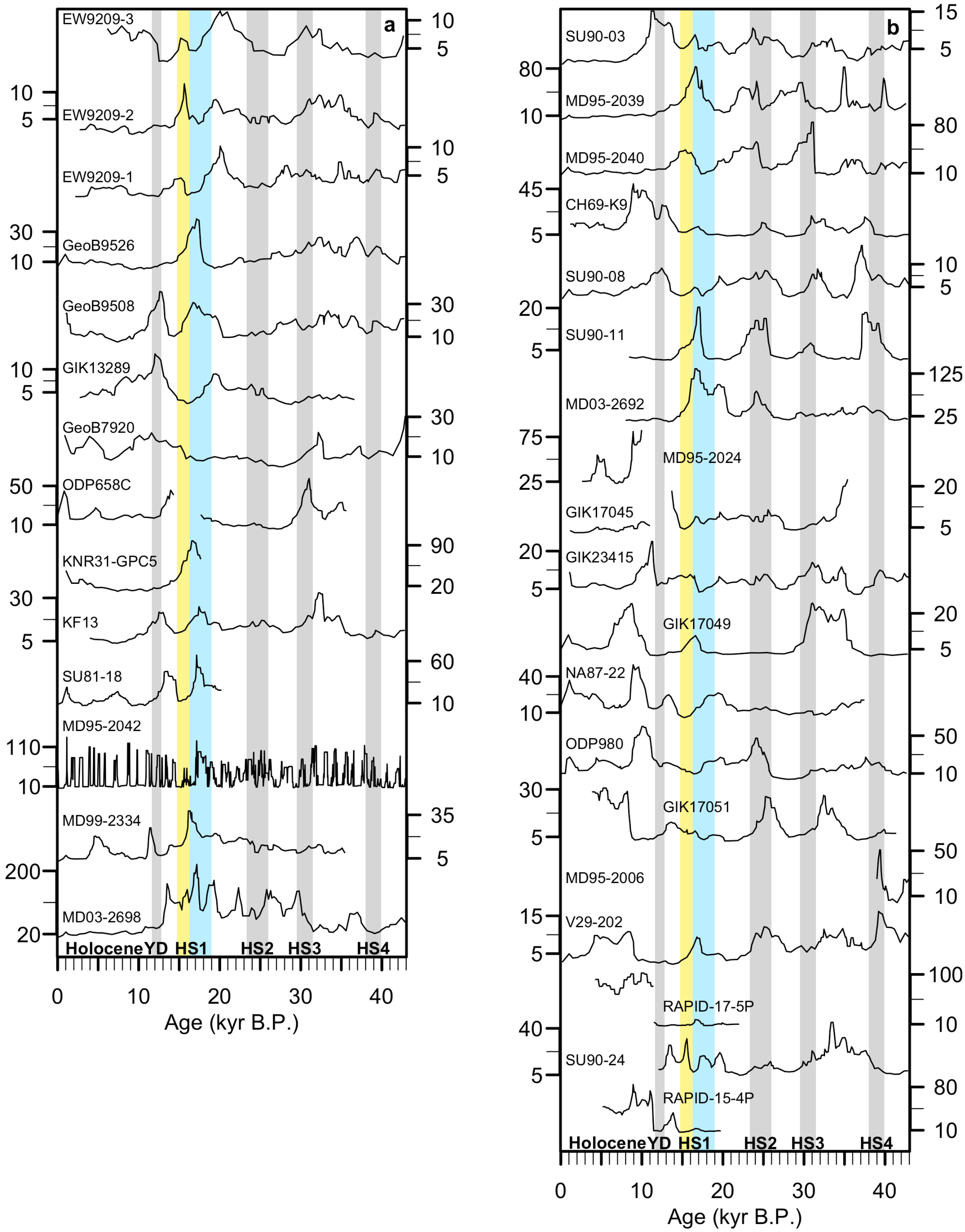
a
EW9209-3
EW9209-2
EW9209-1
GeoB9526
GeoB9508
GIK13289
GeoB7920
ODP658C
KNR31-GPC5
KF13
SU81-18
MD95-2042
MD99-2334
MD03-2698
Holocene YD HS1 HS2 HS3 HS4
Age (kyr B.P.)
b
SU90-03
MD95-2039
MD95-2040
CH69-K9
SU90-08
SU90-11
MD03-2692
MD95-2024
GIK17045
GIK23415
GIK17049
NA87-22
ODP980
GIK17051
MD95-2006
V29-202
RAPID-17-5P
SU90-24
RAPID-15-4P
Holocene YD HS1 HS2 HS3 HS4
Age (kyr B.P.)

730

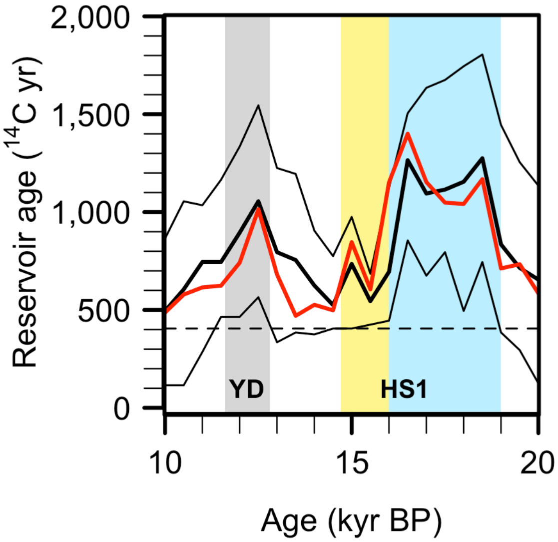

Figure S9: The effect of low sedimentation rate sites on average HLNA reservoir ages. The red line shows average HLNA reservoir ages calculated using only high sedimentation rate sites (see Section 9 in the auxiliary materials for details). The bold black line is our actual HLNA reservoir age history using all sites, thin black lines are the 95% confidence limits, and the dashed line indicates the modern global average reservoir age of 405 ^{14}C yr. Vertical bars as in Fig. S2.

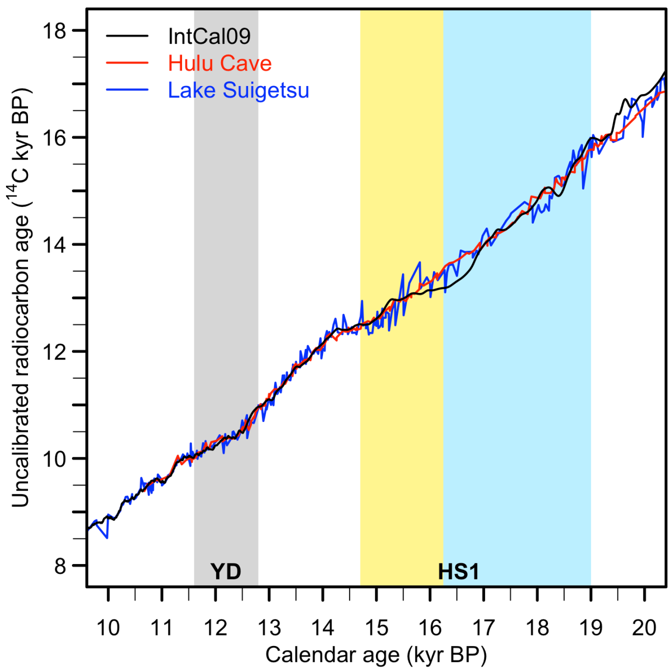

Figure S10: Comparison between IntCal09 [*Reimer et al.*, 2009], Hulu Cave [*Southon et al.*, 2012], and Lake Suigetsu [*Ramsey et al.*, 2012] uncalibrated ^{14}C ages over the last deglaciation. Near the early-late HS1 boundary, younger ages (by up to about 400 ^{14}C yr) in IntCal09 are due to the inclusion of dates from Cariaco Basin, where the local reservoir age may have been overestimated. Vertical bars as in Fig. S2.

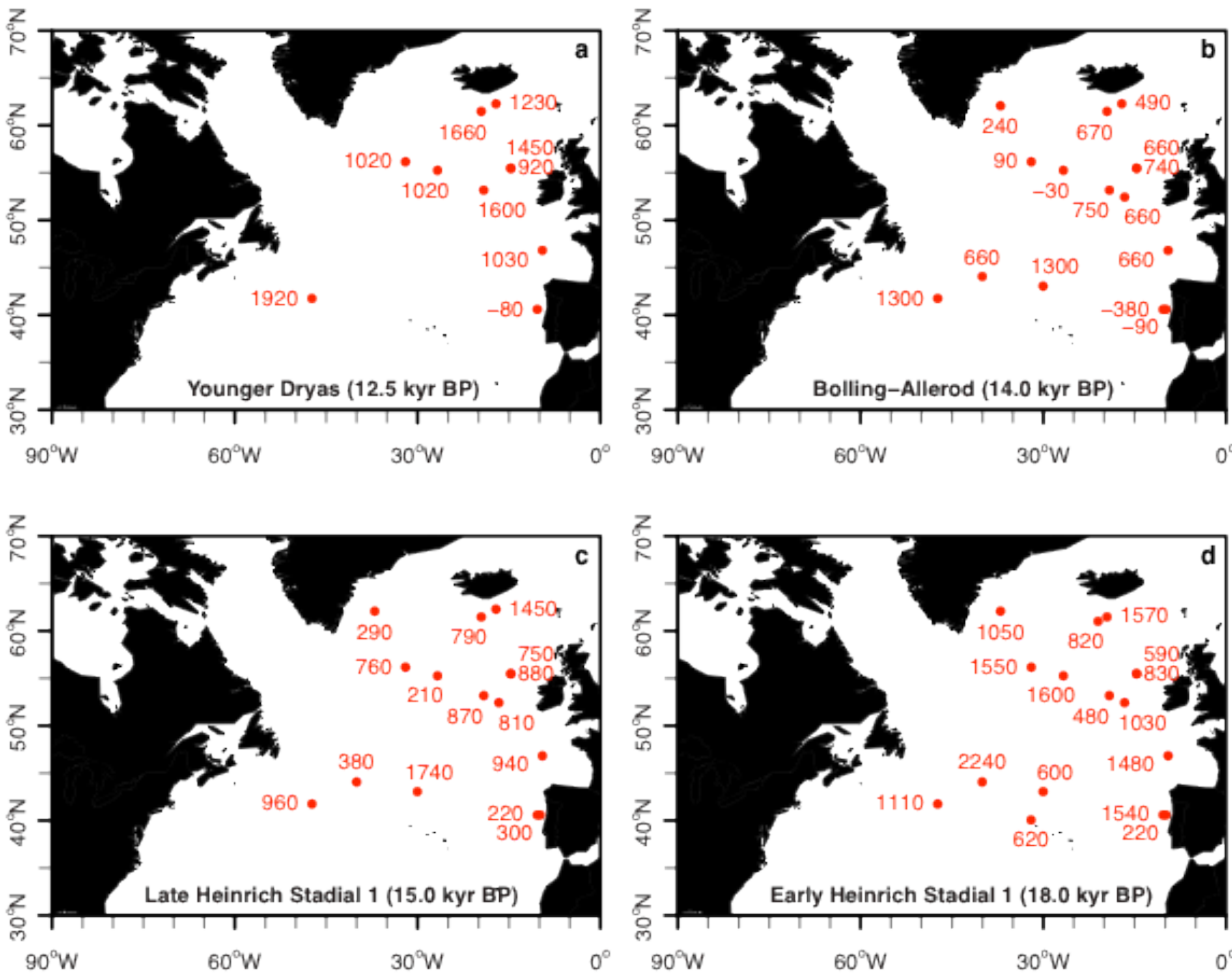

Figure S11: Reservoir ages (in units of ^{14}C yr) calculated for the individual cores used in this study, for select time slices: (a) 12.5 kyr BP, (b) 14.0 kyr BP, (c) 15.0 kyr BP, and (d) 18.0 kyr BP. The wide distribution of reservoir ages within individual times slices is likely the result of larger uncertainties for radiocarbon age models from individual records, records with different temporal resolution, spatial variability of reservoir ages within the HLNA, and potentially small alignment errors resulting from slightly diachronous benthic δ^{18}O changes within the deep North Atlantic.

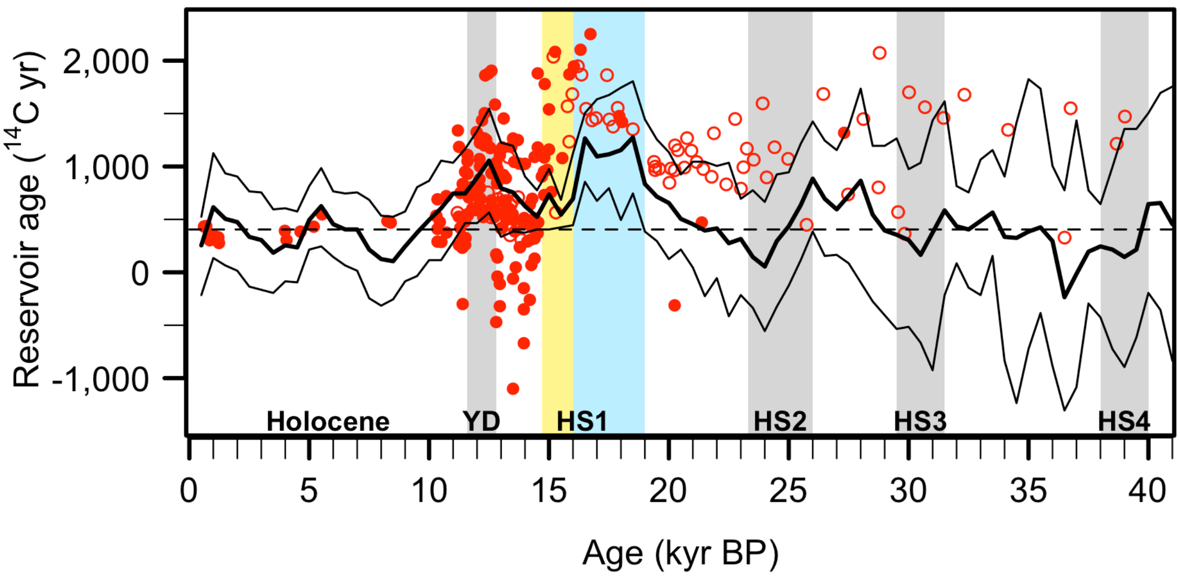

Figure S12: Compilation of high-latitude North Atlantic (HLNA) reservoir age estimates for the last 41 kyr. Our regionally averaged HLNA reservoir ages (thick black line) with 95% confidence intervals (thin black lines) on our low-latitude ^{14}C age model and the dashed line at 405 ^{14}C yr are shown as in Figure 1. Filled red circles indicate HLNA reservoir age estimates from previous studies [*Bard et al.*, 1994; *Austin et al.*, 1995; *Waelbroeck et al.*, 2001; *Björck et al.*, 2003; *Bondevik et al.*, 2006; *Ascough et al.*, 2007, 2009; *Thornalley et al.*, 2011c]. Open red circles indicate estimates reported in calendar years [*Knutz et al.*, 2007; *Peck et al.*, 2007; *Hall et al.*, 2011; *Stanford et al.*, 2011] and intermediate water ages interpreted as surface ages [*Cao et al.*, 2007]. Uncertainty estimates from previous studies have been omitted for clarity. Vertical bars as in Figure S2.

Table S1: Locations and data references for the cores used in this study.

Core	Latitude (°N)	Longitude (°W)	Depth (m)	References
EW9209-3JPC	5.31	44.26	3288	[*Curry et al.*, 1999; *Ostermann and Curry*, 2000]
EW9209-2JPC	5.64	44.47	3528	[*Curry et al.*, 1999; *Ostermann and Curry*, 2000]
EW9209-1JPC	5.91	44.20	4056	[*Curry and Oppo*, 1997; *Curry et al.*, 1999; *Ostermann and Curry*, 2000]
GeoB9526	12.44	18.06	3223	[*Zarriess and Mackensen*, 2010, 2011; *Zarriess et al.*, 2011]
GeoB9508-5	15.50	17.95	2384	[*Mulitza et al.*, 2008]
GIK13289-2	18.07	18.01	2485	[*Sarnthein et al.*, 1994]
GeoB7920-2	20.75	18.58	2278	[*Tjallingii et al.*, 2008; *Collins et al.*, 2011]
ODP658C	20.75	18.58	2273	[*deMenocal et al.*, 2000]
KNR31-GPC5	33.69	57.63	4583	[*Keigwin and Jones*, 1989, 1994; *Keigwin et al.*, 1991]
KF13	37.58	31.84	2690	[*Richter*, 1998]
SU81-18	37.77	10.18	3135	[*Bard et al.*, 1987b, 2000; *Waelbroeck et al.*, 2001; *Gherardi et al.*, 2005]
MD99-2334	37.80	10.17	3146	[*Skinner et al.*, 2003; *Skinner and Shackleton*, 2004, 2005]
MD95-2042	37.80	10.17	3146	[*Shackleton et al.*, 2000, 2004; *Bard et al.*, 2004; *Thouveny et al.*, 2004; *Eynaud et al.*, 2009]
MD03-2698	38.24	10.39	4602	[*Lebreiro et al.*, 2009]
SU90-03	40.05	32.00	2475	[*Chapman et al.*, 2000]
MD95-2040	40.58	9.86	2465	[*de Abreu et al.*, 2003; *Schönfeld et al.*, 2003; *Thouveny et al.*, 2004]
MD95-2039	40.58	10.35	3381	[*Thomson et al.*, 1999, 2000; *Schönfeld et al.*, 2003; *Thouveny et al.*, 2004]
CH69-K9	41.75	47.35	4100	[*Labeyrie et al.*, 1999; *Waelbroeck et al.*, 2001]
SU90-08	43.05	30.04	3080	[*Grousset et al.*, 1993; *Cortijo*, 1995; *Labeyrie et al.*, 1995]
SU90-11	44.07	40.02	3645	[*Labeyrie et al.*, 1995; *Jullien et al.*, 2006]
MD03-2692	46.83	9.52	4064	[*Mojtahid et al.*, 2005; *Eynaud et al.*, 2007; *Toucanne et al.*, 2009]
MD95-2024	50.21	45.69	3448	[*Hoogakker et al.*, 2011]
GIK17045	52.43	16.67	3663	[*Sarnthein et al.*, 1994]
GIK23415-9	53.18	19.15	2472	[*Jung*, 1996; *Weinelt et al.*, 2003]
GIK17049-6	55.26	26.73	3331	[*Sarnthein et al.*, 1994; *Jung*, 1996]

NA87-22	55.48	14.68	2161	[*Duplessy et al.*, 1992; *Labeyrie et al.*, 1995; *Cortijo et al.*, 1997; *Vidal et al.*, 1997; *Waelbroeck et al.*, 2001]
ODP980	55.49	14.7	2168	[*McManus et al.*, 1999; *Oppo et al.*, 2003; *Benway et al.*, 2010]
GIK17051	56.16	31.99	2295	[*Sarnthein et al.*, 1994; *Jung*, 1996]
MD95-2006	57.03	10.06	2130	[*Wilson and Austin*, 2002; *Austin et al.*, 2004; *Dickson et al.*, 2008]
V29-202	61.00	21.00	2658	[*Oppo and Lehman*, 1995]
RAPID-17-5P	61.48	19.54	2303	[*Thornalley et al.*, 2010a, 2010b, 2011b]
SU90-24	62.07	37.03	2100	[*Elliot et al.*, 1998, 2002]
RAPID-15-4P	62.29	17.13	2133	[*Thornalley et al.*, 2010a, 2011b]

Table S2: Reservoir ages for individual HLNA cores at select time slices. Time slices are labeled along the top of the columns, in kyr BP on our low-latitude ^{14}C age model. All reservoir ages are reported in units of ^{14}C yr. Our average HLNA reservoir ages are given in the last row.

Core	12.5	14	15	16	17	18	19	20	21
SU90-03	-	-	-	-	750	620	970	500	330
MD95-2040	-	-90	300	660	720	220	-570	-440	-410
MD95-2039	-80	-380	220	420	890	1540	1070	550	310
CH69-K9	1920	1300	960	820	710	1110	840	610	420
SU90-08	-	1440	1740	1750	1450	600	270	400	400
SU90-11	-	660	380	410	1340	2240	1200	560	130
MD03-2692	1030	660	940	1310	1460	1480	500	400	430
GIK17045	-	660	810	460	750	1030	670	920	640
GIK23415-9	1600	750	870	700	870	480	-30	260	330
GIK17049-6	1020	-30	210	270	1260	1600	1240	1100	830
NA87-22	920	740	880	620	990	830	1200	1150	1380
ODP980	1450	660	750	1530	1200	590	-20	320	330
GIK17051	1020	90	760	1020	1430	1550	1330	-	-
V29-202	-	-	-	400	690	820	860	1060	950
RAPID-17-5P	1660	670	790	-	-	1570	480	40	-140
SU90-24	-	240	290	600	740	1050	910	1930	2060
RAPID-15-4P	1230	490	1450	1690	2020	-	-	-	-
Average HLNA	1060	630	740	690	1090	1150	840	660	460

Table S3: Calculated sea surface temperature (SST) leads over rapid Greenland warmings and reservoir ages for the Heinrich Stadial 1/Bølling-Allerød (HS1/BA) transition, identified by the midpoint of temperature change. Table entries in red are from this study. Parenthetical uncertainty estimates for reservoir ages calculated in this study are 95% confidence intervals.

Record	Latitude (°N)	Longitude (°W)	Age of the midpoint (kyr B.P.)	SST lead (kyr)	Reservoir age (^{14}C yr)	Reference
GRIP/ GISP2	~ 72.5	~ 38	14.53 ± 0.53			[*Waelbroeck et al.*, 2001]
NGRIP (GICC05)	75.1	42.3	14.62 ± 0.185			[*Rasmussen et al.*, 2006]
NA87-22	55.48	14.68	16.44 ± 0.49	1.94 ± 0.75	1880 ± 750	[*Waelbroeck et al.*, 2001]
NA87-22	55.48	14.68	16.25 ± 1.09	1.63 ± 1.09	1100 (770, 1960)	This study
CH69-K9	41.75	47.35	15.73 ± 0.22	1.23 ± 0.60	1180 ± 630	[*Waelbroeck et al.*, 2001]
CH69-K9	41.75	47.35	16.02 ± 0.83	1.39 ± 0.84	1060 (760, 1260)	This study
SU81-18	37.77	10.18	14.87 ± 0.47	0.37 ± 0.74		[*Waelbroeck et al.*, 2001]
SU81-18	37.77	10.18	14.99 ± 0.47	0.37 ± 0.52		This study

Table S4: Low-latitude ^{14}C age model, regionally averaged high-latitude North Atlantic reservoir ages, and ice-rafted debris stack, with calculated uncertainties.

Age (kyr B.P.)	Age model lower 95% limit (kyr B.P.)	Age model upper 95% limit (kyr B.P.)	Reservoir age (^{14}C yr)	Reservoir age lower 95% limit (^{14}C yr)	Reservoir age upper 95% limit (^{14}C yr)	IRD stack (normalized units)	IRD stack σ (normalized units)
0.0	-	-	-	-	-	0.012	0.025
0.5	0.00	1.39	250	-210	520	0.002	0.002
1.0	0.86	1.51	610	130	1120	0.037	0.072
1.5	1.28	2.01	510	70	940	0.001	0.002
2.0	1.69	2.48	470	20	910	0.002	0.004
2.5	2.18	3.03	340	-130	770	0.017	0.029
3.0	2.58	3.47	300	-170	760	0	0
3.5	3.14	3.95	180	-200	600	0.004	0.008
4.0	3.64	4.32	250	-90	600	0.011	0.022
4.5	4.10	4.78	230	-90	580	0.005	0.01
5.0	4.59	5.26	490	220	820	0.011	0.021
5.5	5.13	5.72	620	250	990	0.008	0.011
6.0	5.74	6.28	460	150	770	0.011	0.011
6.5	6.25	6.86	410	60	750	0.016	0.019
7.0	6.68	7.37	410	10	750	0.009	0.011
7.5	7.22	7.83	210	-240	690	0.012	0.015
8.0	7.71	8.33	120	-310	540	0.008	0.014
8.5	8.23	8.80	100	-250	530	0.009	0.012
9.0	8.73	9.35	240	-90	570	0.017	0.018
9.5	9.22	9.85	380	-40	800	0.011	0.018
10.0	9.73	10.37	490	120	860	0.014	0.02
10.5	10.18	10.84	610	120	1060	0.018	0.023
11.0	10.66	11.34	740	280	1030	0.033	0.033
11.5	11.17	11.85	750	470	1170	0.054	0.061
12.0	11.63	12.32	900	470	1340	0.069	0.085
12.5	12.06	12.72	1060	560	1550	0.059	0.083
13.0	12.65	13.27	790	330	1220	0.056	0.067
13.5	13.19	13.77	760	380	1190	0.068	0.078
14.0	13.77	14.29	630	380	900	0.06	0.072
14.5	14.24	14.78	530	400	770	0.116	0.13
15.0	14.76	15.36	740	410	980	0.239	0.21
15.5	15.28	15.88	550	430	680	0.312	0.246

16.0	15.78	16.38	690	450	1130	0.434	0.223
16.5	16.21	16.82	1260	850	1500	0.253	0.254
17.0	16.69	17.28	1090	680	1630	0.29	0.312
17.5	17.15	17.73	1120	790	1680	0.162	0.223
18.0	17.67	18.27	1150	500	1750	0.137	0.184
18.5	18.14	18.74	1270	740	1800	0.066	0.104
19.0	18.69	19.26	840	380	1450	0.172	0.211
19.5	19.28	19.82	720	290	1250	0.138	0.169
20.0	19.78	20.41	660	130	1140	0.064	0.093
20.5	20.19	20.94	500	220	920	0.102	0.134
21.0	20.63	21.41	460	40	1040	0.135	0.181
21.5	21.08	21.89	400	-220	1040	0.071	0.078
22.0	21.53	22.35	420	-50	1010	0.079	0.083
22.5	22.08	22.86	270	-410	1030	0.095	0.157
23.0	22.62	23.39	310	-210	690	0.12	0.157
23.5	23.12	23.88	150	-340	780	0.15	0.174
24.0	23.70	24.45	60	-550	670	0.318	0.278
24.5	24.13	24.98	300	-330	920	0.508	0.288
25.0	24.60	25.60	440	-130	940	0.437	0.279
25.5	25.01	26.03	630	110	1210	0.281	0.268
26.0	25.36	26.51	880	390	1430	0.145	0.144
26.5	25.94	26.96	700	150	1240	0.121	0.119
27.0	26.42	27.44	590	160	1150	0.101	0.118
27.5	26.85	27.92	730	80	1380	0.129	0.14
28.0	27.50	28.40	860	-100	1730	0.039	0.052
28.5	28.08	28.98	540	-280	1200	0.054	0.076
29.0	28.61	29.58	390	-410	1200	0.08	0.117
29.5	29.00	29.98	360	-530	1260	0.116	0.187
30.0	29.47	30.48	300	-510	970	0.148	0.199
30.5	30.08	31.04	170	-660	1040	0.204	0.194
31.0	30.64	31.60	370	-930	1430	0.171	0.177
31.5	31.10	32.14	590	-210	1620	0.127	0.168
32.0	31.62	32.73	430	80	810	0.122	0.138
32.5	32.02	33.27	400	-150	760	0.12	0.121
33.0	32.42	33.76	480	-220	1060	0.125	0.159
33.5	32.88	34.23	570	160	1160	0.129	0.105
34.0	33.26	34.97	330	-830	910	0.102	0.111
34.5	33.72	35.51	330	-1230	1420	0.062	0.071
35.0	34.16	35.96	390	-720	1830	0.121	0.241
35.5	34.59	36.41	430	-390	1730	0.065	0.107

36.0	35.09	36.91	300	-890	1000	0.081	0.113
36.5	35.60	37.41	-230	-1310	780	0.055	0.067
37.0	36.10	37.89	-20	-1080	1430	0.074	0.073
37.5	36.78	38.19	190	-300	770	0.18	0.162
38.0	37.31	38.78	240	-420	650	0.3	0.228
38.5	37.79	39.20	220	-720	990	0.497	0.299
39.0	38.09	40.05	140	-890	1360	0.638	0.234
39.5	38.49	40.45	220	-610	1360	0.47	0.268
40.0	38.93	40.88	650	-200	1510	0.134	0.14
40.5	39.30	41.23	650	-360	1690	0.091	0.101
41.0	39.88	41.74	450	-830	1760	0.069	0.07
41.5	40.48	42.21	-	-	-	0.117	0.163
42.0	40.89	42.93	-	-	-	0.096	0.107
42.5	41.48	43.63	-	-	-	0.206	0.245
43.0	41.93	44.14	-	-	-	0.106	0.178

References:

Ascough, P. L., G. T. Cook, A. J. Dugmore, and E. M. Scott (2007), The North Atlantic marine reservoir effect in the Early Holocene: Implications for defining and understanding MRE values, *Nucl. Instruments Methods Phys. Res. Sect. B Beam Interactions Mater. Atoms*, *259*(1), 438–447, doi:10.1016/j.nimb.2007.01.185.

Ascough, P. L., G. T. Cook, and A. J. Dugmore (2009), North Atlantic marine ^{14}C reservoir effects: Implications for late-Holocene chronological studies, *Quat. Geochronol.*, *4*(3), 171–180, doi:10.1016/j.quageo.2008.12.002.

Austin, W. E., E. Bard, J. B. Hunt, D. Kroon, and J. D. Peacock (1995), The ^{14}C age of the Icelandic Vedde Ash: implications for Younger Dryas marine reservoir age corrections, *Radiocarbon*, *37*(1), 53–62.

Austin, W. E. N., L. J. Wilson, and J. B. Hunt (2004), The age and chronostratigraphical significance of North Atlantic Ash Zone II, *J. Quat. Sci.*, *19*(2), 137–146, doi:10.1002/jqs.821.

Austin, W. E. N., R. J. Telford, U. S. Ninnemann, L. Brown, L. J. Wilson, D. P. Small, and C. L. Bryant (2011), North Atlantic reservoir ages linked to high Younger Dryas atmospheric radiocarbon concentrations, *Glob. Planet. Change*, *79*(3-4), 226–233, doi:10.1016/j.gloplacha.2011.06.011.

Bard, E. (1988), Correction of accelerator mass spectrometry ^{14}C ages measured in planktonic foraminifera: paleoceanographic implications, *Paleoceanography*, *3*(6), 635–645, doi:10.1029/PA003i006p00635.

Bard, E., M. Arnold, J. Duprat, J. Moyes, and J. C. Duplessy (1987a), Reconstruction of the last deglaciation: Deconvolved records of $\delta^{18}O$ profiles, micropaleontological variations and accelerator mass spectrometric ^{14}C dating, *Clim. Dyn.*, *1*(2), 101–112.

Bard, E., M. Arnold, P. Maurice, J. Duprat, J. Moyes, and J.-C. Duplessy (1987b), Retreat velocity of the North Atlantic polar front during the last deglaciation determined by ^{14}C accelerator mass spectrometry, *Nature*, *328*(6133), 791–794, doi:10.1038/328791a0.

Bard, E., M. Arnold, J. Mangerud, M. Paterne, L. Labeyrie, J. Duprat, M.-A. Mélières, E. Sønstegaard, and J.-C. Duplessy (1994), The North Atlantic atmosphere-sea surface ^{14}C gradient during the Younger Dryas climatic event, *Earth Planet. Sci. Lett.*, *126*(4), 275–287, doi:10.1016/0012-821X(94)90112-0.

Bard, E., F. Rostek, J. Turon, and S. Gendreau (2000), Hydrological impact of Heinrich events in the subtropical northeast Atlantic, *Science*, *289*(5483), 1321–1324, doi:10.1126/science.289.5483.1321.

Bard, E., F. Rostek, and G. Ménot-Combes (2004), Radiocarbon calibration beyond 20,000 ^{14}C yr B.P. by means of planktonic foraminifera of the Iberian Margin, *Quat. Res.*, *61*(2), 204–214, doi:10.1016/j.yqres.2003.11.006.

Barker, S., W. Broecker, E. Clark, and I. Hajdas (2007), Radiocarbon age offsets of foraminifera resulting from differential dissolution and fragmentation within the sedimentary bioturbated zone, *Paleoceanography*, *22*(2), PA2205, doi:10.1029/2006PA001354.

Barker, S., P. Diz, M. J. Vautravers, J. Pike, G. Knorr, I. R. Hall, and W. S. Broecker (2009), Interhemispheric Atlantic seesaw response during the last deglaciation, *Nature*, *457*(7233), 1097–1102, doi:10.1038/nature07770.

Benway, H. M., J. F. McManus, D. W. Oppo, and J. L. Cullen (2010), Hydrographic changes in the eastern subpolar North Atlantic during the last deglaciation, *Quat. Sci. Rev.*, *29*(23-24), 3336–3345, doi:10.1016/j.quascirev.2010.08.013.

Björck, S., N. Koç, and G. Skog (2003), Consistently large marine reservoir ages in the Norwegian Sea during the Last Deglaciation, *Quat. Sci. Rev.*, *22*(5-7), 429–435, doi:10.1016/S0277-3791(03)00002-7.

Bond, G. C., and R. Lotti (1995), Iceberg discharges into the North Atlantic on millennial time scales during the last glaciation, *Science*, *267*(5200), 1005–1010, doi:10.1126/science.267.5200.1005.

Bondevik, S., J. Mangerud, H. Birks, S. Gulliksen, and P. Reimer (2006), Changes in North Atlantic radiocarbon reservoir ages during the Allerod and Younger Dryas, *Science*, *312*(5779), 1514–1517, doi:10.1126/science.1123300.

Bouimetarhan, I., M. Prange, E. Schefuß, L. Dupont, J. Lippold, S. Mulitza, and K. Zonneveld (2012), Sahel megadrought during Heinrich Stadial 1: evidence for a three-phase evolution of the low- and mid-level West African wind system, *Quat. Sci. Rev.*, *58*, 66–76, doi:10.1016/j.quascirev.2012.10.015.

Broecker, W., S. Barker, E. Clark, I. Hajdas, and G. Bonani (2006), Anomalous radiocarbon ages for foraminifera shells, *Paleoceanography*, *21*(2), PA2008, doi:10.1029/2005PA001212.

Broecker, W. S., and S. Barker (2007), A 190‰ drop in atmosphere's $\Delta^{14}C$ during the "Mystery Interval" (17.5 to 14.5 kyr), *Earth Planet. Sci. Lett.*, *256*(1-2), 90–99, doi:10.1016/j.epsl.2007.01.015.

Broecker, W. S., D. McGee, K. D. Adams, H. Cheng, R. L. Edwards, C. G. Oviatt, and J. Quade (2009), A Great Basin-wide dry episode during the first half of the Mystery Interval?, *Quat. Sci. Rev.*, *28*(25-26), 2557–2563, doi:10.1016/j.quascirev.2009.07.007.

Butzin, M., M. Prange, and G. Lohmann (2005), Radiocarbon simulations for the glacial ocean: The effects of wind stress, Southern Ocean sea ice and Heinrich events, *Earth Planet. Sci. Lett.*, *235*(1-2), 45–61, doi:10.1016/j.epsl.2005.03.003.

Butzin, M., M. Prange, and G. Lohmann (2012), Readjustment of glacial radiocarbon chronologies by self-consistent three-dimensional ocean circulation modeling, *Earth Planet. Sci. Lett.*, *317-318*, 177–184, doi:10.1016/j.epsl.2011.11.046.

Cao, L., R. G. Fairbanks, R. A. Mortlock, and M. J. Risk (2007), Radiocarbon reservoir age of high latitude North Atlantic surface water during the last deglacial, *Quat. Sci. Rev.*, *26*(5-6), 732–742, doi:10.1016/j.quascirev.2006.10.001.

Channell, J. E. T., C. Xuan, and D. A. Hodell (2009), Stacking paleointensity and oxygen isotope data for the last 1.5 Myr (PISO-1500), *Earth Planet. Sci. Lett.*, *283*(1-4), 14–23, doi:10.1016/j.epsl.2009.03.012.

Chapman, M. R., and N. J. Shackleton (1998), Millennial-scale fluctuations in North Atlantic heat flux during the last 150,000 years, *Earth Planet. Sci. Lett.*, *159*(1), 57–70, doi:10.1016/S0012-821X(98)00068-5.

Chapman, M. R., N. J. Shackleton, and J.-C. Duplessy (2000), Sea surface temperature variability during the last glacial–interglacial cycle: assessing the magnitude and pattern of climate change in the North Atlantic, *Palaeogeogr. Palaeoclim. Palaeoecol.*, *157*(1), 1–25, doi:10.1016/S0031-0182(99)00168-6.

Clark, P. U., A. S. Dyke, J. D. Shakun, A. E. Carlson, J. Clark, B. Wohlfarth, J. X. Mitrovica, S. W. Hostetler, and A. M. McCabe (2009), The Last Glacial Maximum, *Science*, *325*(5941), 710–714, doi:10.1126/science.1172873.

Collins, J. A. et al. (2011), Interhemispheric symmetry of the tropical African rainbelt over the past 23,000 years, *Nat. Geosci.*, *4*(1), 42–45, doi:10.1038/ngeo1039.

Cortijo, E. (1995), La variabilite climatique rapide dans l’Atlantique Nord depuis 128000 ans: relations entre les calottes de glace et l’ocean de surface, Ph. D. thesis, Univ. de Paris-Sud, Paris, France.

Cortijo, E., L. Labeyrie, L. Vidal, M. Vautravers, M. Chapman, J.-C. Duplessy, M. Elliot, M. Arnold, J.-L. Turon, and G. Auffret (1997), Changes in sea surface hydrology associated with Heinrich event 4 in the North Atlantic Ocean between 40° and 60°N, *Earth Planet. Sci. Lett.*, *146*(1), 29–45.

Curry, W., and D. Oppo (1997), Synchronous, high-frequency oscillations in tropical sea surface temperatures and North Atlantic Deep Water production during the last glacial cycle, *Paleoceanography*, *12*(1), 1–14, doi:10.1029/96PA02413.

Curry, W. B., and D. W. Oppo (2005), Glacial water mass geometry and the distribution of $\delta^{13}C$ of ΣCO_2 in the western Atlantic Ocean, *Paleoceanography*, *20*(1), PA1017, doi:10.1029/2004PA001021.

Curry, W. B., T. M. Marchitto, J. F. McManus, D. W. Oppo, and K. L. Laarkamp (1999), Millennial-scale changes in ventilation of the thermocline, intermediate, and deep waters of the glacial North Atlantic, *Geophys. Monogr. Ser.*, *112*, 59–76.

De Abreu, L., N. J. Shackleton, J. Schönfeld, M. Hall, and M. Chapman (2003), Millennial-scale oceanic climate variability off the Western Iberian margin during the last two glacial periods, *Mar. Geol.*, *196*(1-2), 1–20, doi:10.1016/S0025-3227(03)00046-X.

Delaygue, G., T. F. Stocker, F. Joos, and G.-K. Plattner (2003), Simulation of atmospheric radiocarbon during abrupt oceanic circulation changes: trying to reconcile models and reconstructions, *Quat. Sci. Rev.*, *22*(15-17), 1647–1658, doi:10.1016/S0277-3791(03)00171-9.

deMenocal, P., J. Ortiz, T. Guilderson, J. Adkins, M. Sarnthein, L. Baker, and M. Yarusinsky (2000), Abrupt onset and termination of the African Humid Period: rapid climate responses to gradual insolation forcing, *Quat. Sci. Rev.*, *19*(1), 347–361, doi:10.1016/S0277-3791(99)00081-5.

Denton, G. H., W. S. Broecker, and R. B. Alley (2006), The mystery interval 17.5 to 14.5 kyrs ago, *Pages News*, *14*, 14–16.

Denton, G. H., R. F. Anderson, J. R. Toggweiler, R. L. Edwards, J. M. Schaefer, and A. E. Putnam (2010), The Last Glacial Termination, *Science*, *328*(5986), 1652–1656, doi:10.1126/science.1184119.

Dickson, A. J., W. E. N. Austin, I. R. Hall, M. A. Maslin, and M. Kucera (2008), Centennial-scale evolution of Dansgaard-Oeschger events in the northeast Atlantic Ocean between 39.5 and 56.5 ka B.P., *Paleoceanography*, *23*(3), PA3206, doi:10.1029/2008PA001595.

Duplessy, J.-C., L. Labeyrie, M. Arnold, M. Paterne, J. Duprat, and T. van Weering (1992), Changes in the surface salinity of the North Atlantic ocean during the last deglaciation, *Nature*, *358*(6386), 485–488, doi:10.1038/358485a0.

Elliot, M., L. Labeyrie, G. Bond, E. Cortijo, J. Turon, N. Tisnerat, and J. Duplessy (1998), Millennial-scale iceberg discharges in the Irminger Basin during the last glacial period: Relationship with the Heinrich events and environmental settings, *Paleoceanography*, *13*(5), 433–446, doi:10.1029/98PA01792.

Elliot, M., L. Labeyrie, and J.-C. Duplessy (2002), Changes in North Atlantic deep-water formation associated with the Dansgaard–Oeschger temperature oscillations (60–10 ka), *Quat. Sci. Rev.*, *21*(10), 1153–1165, doi:10.1016/S0277-3791(01)00137-8.

Eynaud, F., S. Zaragosi, J. D. Scourse, M. Mojtahid, J. F. Bourillet, I. R. Hall, A. Penaud, M. Locascio, and A. Reijonen (2007), Deglacial laminated facies on the NW European continental margin: The hydrographic significance of British-Irish Ice Sheet deglaciation and Fleuve Manche paleoriver discharges, *Geochem. Geophys. Geosystems*, *8*(6), Q06019, doi:10.1029/2006GC001496.

Eynaud, F. et al. (2009), Position of the Polar Front along the western Iberian margin during key cold episodes of the last 45 ka, *Geochem. Geophys. Geosystems*, *10*(7), Q07U05, doi:10.1029/2009GC002398.

Fairbanks, R. G., R. A. Mortlock, T.-C. Chiu, L. Cao, A. Kaplan, T. P. Guilderson, T. W. Fairbanks, A. L. Bloom, P. M. Grootes, and M.-J. Nadeau (2005), Radiocarbon calibration curve spanning 0 to 50,000 years BP based on paired ^{230}Th/^{234}U/^{238}U and ^{14}C dates on pristine corals, *Quat. Sci. Rev.*, *24*(16-17), 1781–1796, doi:10.1016/j.quascirev.2005.04.007.

Farmer, E. C., A. Kaplan, P. B. de Menocal, and J. Lynch-Stieglitz (2007), Corroborating ecological depth preferences of planktonic foraminifera in the tropical Atlantic with the stable oxygen isotope ratios of core top specimens, *Paleoceanography*, *22*(3), PA3205, doi:10.1029/2006PA001361.

Franke, J., A. Paul, and M. Schulz (2008), Modeling variations of marine reservoir ages during the last 45000 years, *Clim. Past*, *4*, 125–136.

Friedrich, T., and A. Timmermann (2012), Millennial-scale glacial meltwater pulses and their effect on the spatiotemporal benthic δ^{18}O variability, *Paleoceanography*, *27*(3), PA3215, doi:10.1029/2012PA002330.

Ganssen, G., and D. Kroon (2000), The isotopic signature of planktonic foraminifera from NE Atlantic surface sediments: implications for the reconstruction of past oceanic conditions, *J. Geol. Soc. Lond.*, *157*(3), 693–699.

Gherardi, J., L. Labeyrie, J. McManus, R. Francois, L. Skinner, and E. Cortijo (2005), Evidence from the Northeastern Atlantic basin for variability in the rate of the meridional overturning circulation through the last deglaciation, *Earth Planet. Sci. Lett.*, *240*(3-4), 710–723, doi:10.1016/j.epsl.2005.09.061.

Gherardi, J.-M., L. Labeyrie, S. Nave, R. Francois, J. F. McManus, and E. Cortijo (2009), Glacial-interglacial circulation changes inferred from ^{231}Pa/^{230}Th sedimentary record in the North Atlantic region, *Paleoceanography*, *24*(2), PA2201, doi:10.1029/2008PA001696.

Grousset, F., L. Labey, J. Sinko, M. Cremer, G. Bond, J. Duprat, E. Cortijo, and S. Huon (1993), Patterns of ice-rafted detritus in the glacial North Atlantic (40-55°N), *Paleoceanography*, *8*(2), 175–192, doi:10.1029/92PA02923.

Hall, I. R., E. Colmenero-Hidalgo, R. Zahn, V. L. Peck, and S. R. Hemming (2011), Centennial- to millennial-scale ice-ocean interactions in the subpolar northeast Atlantic 18-41 kyr ago, *Paleoceanography*, *26*(2), PA2224, doi:10.1029/2010PA002084.

Hanslik, D., M. Jakobsson, J. Backman, S. Björck, E. Sellén, M. O'Regan, E. Fornaciari, and G. Skog (2010), Quaternary Arctic Ocean sea ice variations and radiocarbon reservoir age corrections, *Quat. Sci. Rev.*, *29*(25-26), 3430–3441, doi:10.1016/j.quascirev.2010.06.011.

Heinrich, H. (1988), Origin and consequences of cyclic ice-rafting in the northeast Atlantic Ocean during the past 130,000 years, *Quat. Res.*, *29*(2), 142–152, doi:10.1016/0033-5894(88)90057-9.

Hemming, S. R. (2004), Heinrich events: Massive late Pleistocene detritus layers of the North Atlantic and their global climate imprint, *Rev. Geophys.*, *42*(1), RG1005, doi:10.1029/2003RG000128.

Hillaire-Marcel, C., and A. de Vernal (2008), Stable isotope clue to episodic sea ice formation in the glacial North Atlantic, *Earth Planet. Sci. Lett.*, *268*(1-2), 143–150, doi:10.1016/j.epsl.2008.01.012.

Hoffmann, D. L., J. W. Beck, D. A. Richards, P. L. Smart, J. S. Singarayer, T. Ketchmark, and C. J. Hawkesworth (2010), Towards radiocarbon calibration beyond 28 ka using speleothems from the Bahamas, *Earth Planet. Sci. Lett.*, *289*(1-2), 1–10, doi:10.1016/j.epsl.2009.10.004.

Hoogakker, B. A. A., M. R. Chapman, I. N. McCave, C. Hillaire-Marcel, C. R. W. Ellison, I. R. Hall, and R. J. Telford (2011), Dynamics of North Atlantic Deep Water masses during the Holocene, *Paleoceanography*, *26*(4), PA4214, doi:10.1029/2011PA002155.

Hughen, K., J. Southon, S. Lehman, C. Bertrand, and J. Turnbull (2006), Marine-derived ^{14}C calibration and activity record for the past 50,000 years updated from the Cariaco Basin, *Quat. Sci. Rev.*, *25*(23-24), 3216–3227, doi:10.1016/j.quascirev.2006.03.014.

Hughen, K. A., M. G. Baillie, E. Bard, J. W. Beck, C. J. Bertrand, P. G. Blackwell, C. E. Buck, G. S. Burr, K. B. Cutler, and P. E. Damon (2004), Marine04 marine radiocarbon age calibration, 0-26 cal kyr BP, *Radiocarbon*, *46*(3), 1059–1086.

Jullien, E., F. E. Grousset, S. R. Hemming, V. L. Peck, I. R. Hall, C. Jeantet, and I. Billy (2006), Contrasting conditions preceding MIS3 and MIS2 Heinrich events, *Glob. Planet. Change*, *54*(3-4), 225–238, doi:10.1016/j.gloplacha.2006.06.021.

Jung, S. (1996), Wassermassenaustausch zwischen NE-Atlantik und Nordmeer wahrend der letzen 300000/80000 Jahre im Abbild stabiler O- und C- Isotope, *Berichte aus dem Sonderforschungsbereich 313*, Christian Albrechts Univ., Kiel.

Keigwin, L., and G. Jones (1994), Western North Atlantic evidence for millennial-scale changes in ocean circulation and climate, *J. Geophys. Res.*, *99*(C6), 12397–12410, doi:10.1029/94JC00525.

Keigwin, L., G. Jones, S. Lehman, and E. Boyle (1991), Deglacial meltwater discharge, North Atlantic deep circulation, and abrupt climate change, *J. Geophys. Res.*, *96*(C9), 16811–16826, doi:10.1029/91JC01624.

Keigwin, L. D., and G. A. Jones (1989), Glacial-Holocene stratigraphy, chronology, and paleoceanographic observations on some North Atlantic sediment drifts, *Deep Sea Res. Part Ocean. Res. Pap.*, *36*(6), 845–867.

Knutz, P. C., R. Zahn, and I. R. Hall (2007), Centennial-scale variability of the British Ice Sheet: Implications for climate forcing and Atlantic meridional overturning circulation during the last deglaciation, *Paleoceanography*, *22*(1), PA1207, doi:10.1029/2006PA001298.

Kromer, B., M. Friedrich, K. Hughen, F. Kaiser, S. Remmele, M. Schaub, and S. Talamo (2004), Late glacial ^{14}C ages from a floating, 1382-ring pine chronology, *Radiocarbon*, *46*(3), 1203–1209.

Labeyrie, L., L. Vidal, E. Cortijo, M. Paterne, M. Arnold, J. C. Duplessy, M. Vautravers, M. Labracherie, J. Duprat, and J. L. Turon (1995), Surface and deep hydrology of the Northern Atlantic Ocean during the past 150000 years, *Philos. Trans. R. Soc. Lond. B. Biol. Sci.*, *348*(1324), 255–264.

Labeyrie, L., H. Leclaire, C. Waelbroeck, E. Cortijo, J.-C. Duplessy, L. Vidal, M. Elliot, B. Le Coat, and G. Auffret (1999), Temporal variability of the surface and deep waters of the North West Atlantic Ocean at orbital and millennial scales, *Geophys. Monogr. Ser.*, *112*, 77–98, doi:10.1029/GM112p0077.

Labeyrie, L., C. Waelbroeck, E. Cortijo, E. Michel, and J.-C. Duplessy (2005), Changes in deep water hydrology during the Last Deglaciation, *Comptes Rendus Geosci.*, *337*(10-11), 919–927, doi:10.1016/j.crte.2005.05.010.

Laj, C., C. Kissel, A. Mazaud, J. Channell, and J. Beer (2000), North Atlantic palaeointensity stack since 75 ka (NAPIS-75) and the duration of the Laschamp event, *Philos. Trans. R. Soc. Lond. Ser. - Math. Phys. Eng. Sci.*, *358*(1768), 1009–1025, doi:10.1098/rsta.2000.0571.

Laj, C., C. Kissel, and J. Beer (2004), High resolution global paleointensity stack since 75 kyr (GLOPIS-75) calibrated to absolute values, *Geophys. Monogr. Ser.*, *145*, 255–265.

Lal, D., and C. Charles (2007), Deconvolution of the atmospheric radiocarbon record in the last 50,000 years, *Earth Planet. Sci. Lett.*, *258*(3-4), 550–560, doi:10.1016/j.epsl.2007.04.016.

Lebreiro, S. M., A. H. L. Voelker, A. Vizcaino, F. G. Abrantes, U. Alt-Epping, S. Jung, N. Thouveny, and E. Gràcia (2009), Sediment instability on the Portuguese continental margin under abrupt glacial climate changes (last 60 kyr), *Quat. Sci. Rev.*, *28*(27-28), 3211–3223, doi:10.1016/j.quascirev.2009.08.007.

Lippold, J., Y. Luo, R. Francois, S. E. Allen, J. Gherardi, S. Pichat, B. Hickey, and H. Schulz (2012), Strength and geometry of the glacial Atlantic Meridional Overturning Circulation, *Nat. Geosci.*, *5*(11), 813–816, doi:10.1038/ngeo1608.

Lisiecki, L. E., and P. A. Lisiecki (2002), Application of dynamic programming to the correlation of paleoclimate records, *Paleoceanography*, *17*(D4), 1049, doi:10.1029/2001PA000733.

Lisiecki, L. E., and M. E. Raymo (2005), A Pliocene-Pleistocene stack of 57 globally distributed benthic $\delta^{18}O$ records, *Paleoceanography*, *20*(1), PA1003, doi:10.1029/2004PA001071.

Lisiecki, L. E., and M. E. Raymo (2009), Diachronous benthic $\delta^{18}O$ responses during late Pleistocene terminations, *Paleoceanography*, *24*(3), PA3210, doi:10.1029/2009PA001732.

Martinson, D. G., N. G. Pisias, J. D. Hays, J. Imbrie, T. C. Moore Jr, and N. J. Shackleton (1987), Age dating and the orbital theory of the ice ages: development of a high-resolution 0 to 300,000-year chronostratigraphy, *Quat. Res.*, *27*(1), 1–29.

McManus, J. F., D. W. Oppo, and J. L. Cullen (1999), A 0.5-Million-Year Record of Millennial-Scale Climate Variability in the North Atlantic, *Science*, *283*(5404), 971–975, doi:10.1126/science.283.5404.971.

Meland, M. Y., T. M. Dokken, E. Jansen, and K. Hevroy (2008), Water mass properties and exchange between the Nordic seas and the northern North Atlantic during the period 23-6 ka: Benthic oxygen isotopic evidence, *Paleoceanography*, *23*(1), PA1210, doi:10.1029/2007PA001416.

Mojtahid, M., F. Eynaud, S. Zaragosi, J. Scourse, J.-F. Bourillet, and T. Garlan (2005), Palaeoclimatology and palaeohydrography of the glacial stages on Celtic and Armorican margins over the last 360000 yrs, *Mar. Geol.*, *224*(1-4), 57–82, doi:10.1016/j.margeo.2005.07.007.

Mulitza, S., M. Prange, J.-B. Stuut, M. Zabel, T. von Dobeneck, A. C. Itambi, J. Nizou, M. Schulz, and G. Wefer (2008), Sahel megadroughts triggered by glacial slowdowns of Atlantic meridional overturning, *Paleoceanography*, *23*(4), PA4206, doi:10.1029/2008PA001637.

Muscheler, R., J. Beer, G. Wagner, C. Laj, C. Kissel, G. Raisbeck, F. Yiou, and P. Kubik (2004), Changes in the carbon cycle during the last deglaciation as indicated by the comparison of Be-10 and C-14 records, *Earth Planet. Sci. Lett.*, *219*(3-4), 325–340, doi:10.1016/S0012-821X(03)00722-2.

Negre, C., R. Zahn, A. L. Thomas, P. Masqué, G. M. Henderson, G. Martínez-Méndez, I. R. Hall, and J. L. Mas (2010), Reversed flow of Atlantic deep water during the Last Glacial Maximum, *Nature*, *468*(7320), 84–88, doi:10.1038/nature09508.

Oppo, D., and S. Lehman (1995), Suborbital timescale variability of North Atlantic Deep Water during the past 200,000 years, *Paleoceanography*, *10*(5), 901–910, doi:10.1029/95PA02089.

Oppo, D., J. McManus, and J. Cullen (2003), Deepwater variability in the Holocene epoch, *Nature*, *422*(6929), 277–278, doi:10.1038/422277b.

Ostermann, D., and W. Curry (2000), Calibration of stable isotopic data: An enriched $\delta^{18}O$ standard used for source gas mixing detection and correction, *Paleoceanography*, *15*(3), 353–360, doi:10.1029/1999PA000411.

Pahnke, K., S. L. Goldstein, and S. R. Hemming (2008), Abrupt changes in Antarctic Intermediate Water circulation over the past 25,000 years, *Nat. Geosci.*, *1*(12), 870–874, doi:10.1038/ngeo360.

Parnell, A. C., J. Haslett, J. R. M. Allen, C. E. Buck, and B. Huntley (2008), A flexible approach to assessing synchroneity of past events using Bayesian reconstructions of sedimentation history, *Quat. Sci. Rev.*, *27*(19-20), 1872–1885, doi:10.1016/j.quascirev.2008.07.009.

Peck, V. L., I. R. Hall, R. Zahn, and J. D. Scourse (2007), Progressive reduction in NE Atlantic intermediate water ventilation prior to Heinrich events: Response to NW European ice sheet instabilities?, *Geochem. Geophys. Geosystems*, *8*, Q01N10, doi:10.1029/2006GC001321.

Pisias, N. G., D. G. Martinson, T. C. Moore, N. J. Shackleton, W. Prell, J. Hays, and G. Boden (1984), High resolution stratigraphic correlation of benthic oxygen isotopic records spanning the last 300,000 years, *Mar. Geol.*, *56*, 119–136.

Primeau, F., and E. Deleersnijder (2009), On the time to tracer equilibrium in the global ocean, *Ocean Sci.*, *5*(1), 13.

Ramsey, C. B. et al. (2012), A Complete Terrestrial Radiocarbon Record for 11.2 to 52.8 kyr B.P., *Science*, *338*(6105), 370–374, doi:10.1126/science.1226660.

Rashid, H., F. Saint-Ange, D. C. Barber, M. E. Smith, and N. Devalia (2012), Fine scale sediment structure and geochemical signature between eastern and western North Atlantic during Heinrich events 1 and 2, *Quat. Sci. Rev.*, *46*, 136–150, doi:10.1016/j.quascirev.2012.04.026.

Rasmussen, S. O. et al. (2006), A new Greenland ice core chronology for the last glacial termination, *J. Geophys. Res.*, *111*, D06102, doi:10.1029/2005JD006079.

Reimer, P. J., M. G. Baillie, E. Bard, A. Bayliss, J. W. Beck, C. J. Bertrand, P. G. Blackwell, C. E. Buck, G. S. Burr, and K. B. Cutler (2004), IntCal04 terrestrial radiocarbon age calibration, 0-26 cal kyr BP, *Radiocarbon*, *46*(3), 1029–1058.

Reimer, P. J. et al. (2009), IntCal09 and Marine09 radiocarbon age calibration curves, 0-50,000 years cal BP, *Radiocarbon*, *51*(4), 1111–1150.

Richter, T. (1998), Sedimentary fluxes at the Mid-Atlantic Ridge - Sediment sources, accumulation rates, and geochemical characterisation, *GEOMAR Report 73*, GEOMAR Research Center for Marine Geosciences, Christian Albrechts University, Kiel.

Ritz, S. P., T. F. Stocker, and S. A. Mueller (2008), Modeling the effect of abrupt ocean circulation change on marine reservoir age, *Earth Planet. Sci. Lett.*, *268*(1-2), 202–211, doi:10.1016/j.epsl.2008.01.024.

Roche, D. M., A. P. Wiersma, and H. Renssen (2010), A systematic study of the impact of freshwater pulses with respect to different geographical locations, *Clim. Dyn.*, *34*(7-8), 997–1013, doi:10.1007/s00382-009-0578-8.

Ruddiman, W. F., and A. McIntyre (1981), The North Atlantic Ocean during the last deglaciation, *Palaeogeogr. Palaeoclim. Palaeoecol.*, *35*, 145–214.

Salgueiro, E., A. H. L. Voelker, L. de Abreu, F. Abrantes, H. Meggers, and G. Wefer (2010), Temperature and productivity changes off the western Iberian margin during the last 150 ky, *Quat. Sci. Rev.*, *29*(5-6), 680–695, doi:10.1016/j.quascirev.2009.11.013.

Sarnthein, M., K. Winn, S. Jung, J. Duplessy, L. Labeyrie, H. Erlenkeuser, and G. Ganssen (1994), Changes in east Atlantic deepwater circulation over the last 30,000 years: Eight time slice reconstructions, *Paleoceanography*, *9*(2), 209–267, doi:10.1029/93PA03301.

Sarnthein, M., P. Grootes, J. Kennett, and M.-J. Nadeau (2007), ^{14}C reservoir ages show deglacial changes in ocean currents and carbon cycle, *Geophys. Monogr. Ser.*, *173*, 175–196, doi:10.1029/173GM13.

Schönfeld, J., R. Zahn, and L. de Abreu (2003), Surface and deep water response to rapid climate changes at the Western Iberian Margin, *Glob. Planet. Change*, *36*(4), 237–264, doi:10.1016/S0921-8181(02)00197-2.

Shackleton, N. J., M. Hall, and E. Vincent (2000), Phase relationships between millennial-scale events 64,000-24,000 years ago, *Paleoceanography*, *15*(6), 565–569, doi:10.1029/2000PA000513.

Shackleton, N. J., R. . Fairbanks, T. Chiu, and F. Parrenin (2004), Absolute calibration of the Greenland time scale: implications for Antarctic time scales and for $\Delta^{14}C$, *Quat. Sci. Rev.*, *23*(14-15), 1513–1522, doi:10.1016/j.quascirev.2004.03.006.

Shackleton, N. J. (1967), Oxygen Isotope Analyses and Pleistocene Temperatures Re-assessed, *Nature*, *215*(5096), 15–17, doi:10.1038/215015a0.

Siberlin, C., and C. Wunsch (2011), Oceanic tracer and proxy time scales revisited, *Clim. Past*, *7*(1), 27–39, doi:10.5194/cp-7-27-2011.

Simstich, J., M. Sarnthein, and H. Erlenkeuser (2003), Paired $\delta^{18}O$ signals of *Neogloboquadrina pachyderma* (s) and *Turborotalita quinqueloba* show thermal stratification structure in Nordic Seas, *Mar. Micropaleontol.*, *48*(1-2), 107–125, doi:10.1016/S0377-8398(02)00165-2.

Singarayer, J. S., D. A. Richards, A. Ridgwell, P. J. Valdes, W. E. N. Austin, and J. W. Beck (2008), An oceanic origin for the increase of atmospheric radiocarbon during the Younger Dryas, *Geophys. Res. Lett.*, *35*(14), L14707, doi:10.1029/2008GL034074.

Skinner, L. C. (2008), Revisiting the absolute calibration of the Greenland ice-core age-scales, *Clim. Past*, *4*(4), 295–302.

Skinner, L. C., and N. J. Shackleton (2004), Rapid transient changes in northeast Atlantic deep water ventilation age across Termination I, *Paleoceanography*, *19*(2), PA2005, doi:10.1029/2003PA000983.

Skinner, L. C., and N. J. Shackleton (2005), An Atlantic lead over Pacific deep-water change across Termination I: implications for the application of the marine isotope stage stratigraphy, *Quat. Sci. Rev.*, *24*(5-6), 571–580, doi:10.1016/j.quascirev.2004.11.008.

Skinner, L. C., N. J. Shackleton, and H. Elderfield (2003), Millennial-scale variability of deep-water temperature and $\delta^{18}O_{dw}$ indicating deep-water source variations in the Northeast Atlantic, 0-34 cal. ka BP, *Geochem. Geophys. Geosystems*, *4*(12), 1098, doi:10.1029/2003GC000585.

Southon, J., A. L. Noronha, H. Cheng, R. L. Edwards, and Y. Wang (2012), A high-resolution record of atmospheric ^{14}C based on Hulu Cave speleothem H82, *Quat. Sci. Rev.*, *33*, 32–41, doi:10.1016/j.quascirev.2011.11.022.

Stanford, J. D., E. J. Rohling, S. Bacon, A. P. Roberts, F. E. Grousset, and M. Bolshaw (2011), A new concept for the paleoceanographic evolution of Heinrich event 1 in the North Atlantic, *Quat. Sci. Rev.*, *30*(9-10), 1047–1066, doi:10.1016/j.quascirev.2011.02.003.

Stocker, T., and D. Wright (1996), Rapid changes in ocean circulation and atmospheric radiocarbon, *Paleoceanography*, *11*(6), 773–795, doi:10.1029/96PA02640.

Svensson, A. et al. (2008), A 60 000 year Greenland stratigraphic ice core chronology, *Clim. Past*, *4*(1), 47–57, doi:10.5194/cp-4-47-2008.

Thomson, J., S. Nixon, C. P. Summerhayes, J. Schönfeld, R. Zahn, and P. Grootes (1999), Implications for sedimentation changes on the Iberian margin over the last two glacial/interglacial transitions from $(^{230}\mathrm{Th}_{excess})_0$ systematics, *Earth Planet. Sci. Lett.*, *165*(3), 255–270.

Thomson, J., S. Nixon, C. Summerhayes, E. Rohling, J. Schonfeld, R. Zahn, P. Grootes, F. Abrantes, L. Gaspar, and S. Vaqueiro (2000), Enhanced productivity on the Iberian margin during glacial/interglacial transitions revealed by barium and diatoms, *J. Geol. Soc. Lond.*, *157*(Part 3), 667–677.

Thornalley, D. J. R., H. Elderfield, and I. N. McCave (2010a), Intermediate and deep water paleoceanography of the northern North Atlantic over the past 21,000 years, *Paleoceanography*, *25*(1), PA1211, doi:10.1029/2009PA001833.

Thornalley, D. J. R., H. Elderfield, and I. N. McCave (2010b), Reconstructing North Atlantic deglacial surface hydrography and its link to the Atlantic overturning circulation, *Glob. Planet. Change*, *79*(3-4), 163–175, doi:10.1016/j.gloplacha.2010.06.003.

Thornalley, D. J. R., I. N. McCave, and H. Elderfield (2011a), Tephra in deglacial ocean sediments south of Iceland: Stratigraphy, geochemistry and oceanic reservoir ages, *J. Quat. Sci.*, *26*(2), 190–198, doi:10.1002/jqs.1442.

Thornalley, D. J. R., S. Barker, W. S. Broecker, H. Elderfield, and I. N. McCave (2011b), The Deglacial Evolution of North Atlantic Deep Convection, *Science*, *331*(6014), 202–205, doi:10.1126/science.1196812.

Thouveny, N., J. Carcaillet, E. Moreno, G. Leduc, and D. Nérini (2004), Geomagnetic moment variation and paleomagnetic excursions since 400 kyr BP: a stacked record from sedimentary sequences of the Portuguese margin, *Earth Planet. Sci. Lett.*, *219*(3-4), 377–396, doi:10.1016/S0012-821X(03)00701-5.

Tjallingii, R., M. Claussen, J.-B. W. Stuut, J. Fohlmeister, A. Jahn, T. Bickert, F. Lamy, and U. Röhl (2008), Coherent high- and low-latitude control of the northwest African hydrological balance, *Nat. Geosci.*, *1*(10), 670–675, doi:10.1038/ngeo289.

Toucanne, S., S. Zaragosi, J. F. Bourillet, M. Cremer, F. Eynaud, B. Van Vliet-Lanoë, A. Penaud, C. Fontanier, J. L. Turon, and E. Cortijo (2009), Timing of massive "Fleuve Manche" discharges over the last 350 kyr: insights into the European ice-sheet oscillations and the European drainage network from MIS 10 to 2, *Quat. Sci. Rev.*, *28*(13-14), 1238–1256, doi:10.1016/j.quascirev.2009.01.006.

Vidal, L., L. Labeyrie, E. Cortijo, M. Arnold, J. C. Duplessy, E. Michel, S. Becque, and T. C. E. Van Weering (1997), Evidence for changes in the North Atlantic Deep Water linked to meltwater surges during the Heinrich events, *Earth Planet. Sci. Lett.*, *146*(1), 13–27.

Vidal, L., R. R. Schneider, O. Marchal, T. Bickert, T. F. Stocker, and G. Wefer (1999), Link between the North and South Atlantic during the Heinrich events of the last glacial period, *Clim. Dyn.*, *15*(12), 909–919, doi:10.1007/s003820050321.

Voelker, A. L., M. Sarnthein, P. M. Grootes, H. Erlenkeuser, C. Laj, A. Mazaud, M. J. Nadeau, and M. Schleicher (1998), Correlation of marine ^{14}C ages from the Nordic Seas with the GISP2 isotope record: implications for ^{14}C calibration beyond 25 ka BP., *Radiocarbon*, *40*(1), 517–534.

Waelbroeck, C., J. Duplessy, E. Michel, L. Labeyrie, D. Paillard, and J. Duprat (2001), The timing of the last deglaciation in North Atlantic climate records, *Nature*, *412*(6848), 724–727, doi:10.1038/35089060.

Waelbroeck, C., L. C. Skinner, L. Labeyrie, J.-C. Duplessy, E. Michel, N. V. Riveiros, J.-M. Gherardi, and F. Dewilde (2011), The timing of deglacial circulation changes in the Atlantic, *Paleoceanography*, *26*, PA3213, doi:10.1029/2010PA002007.

Weinelt, M., A. Rosell-Mele, U. Pflaumann, M. Sarnthein, and T. Kiefer (2003), The role of productivity in the Northeast Atlantic on abrupt climate change over the last 80,000 years, *Z. Dtsch. Geol. Ges.*, *154*, 47–66.

Wilson, L. J., and W. E. N. Austin (2002), Millennial and sub-millennial variability in sediment colour from the Barra Fan, NW Scotland: implications for British ice sheet dynamics, *Spec. Publ. Geol. Soc. Lond.*, *203*, 349–365, doi:10.1144/GSL.SP.2002.203.01.18.

Winsor, K., A. E. Carlson, G. P. Klinkhammer, J. S. Stoner, and R. G. Hatfield (2012), Evolution of the northeast Labrador Sea during the last interglaciation, *Geochem. Geophys. Geosystems*, *13*(11), Q11006, doi:10.1029/2012GC004263.

Wunsch, C., and P. Heimbach (2008), How long to oceanic tracer and proxy equilibrium?, *Quat. Sci. Rev.*, *27*(7-8), 637–651, doi:10.1016/j.quascirev.2008.01.006.

Xie, R. C., F. Marcantonio, and M. W. Schmidt (2012), Deglacial variability of Antarctic Intermediate Water penetration into the North Atlantic from authigenic neodymium isotope ratios, *Paleoceanography*, *27*(3), PA3221, doi:10.1029/2012PA002337.

Yu, J., H. Elderfield, and A. M. Piotrowski (2008), Seawater carbonate ion-$\delta^{13}C$ systematics and application to glacial–interglacial North Atlantic ocean circulation, *Earth Planet. Sci. Lett.*, *271*(1-4), 209–220, doi:10.1016/j.epsl.2008.04.010.

Zarriess, M., and A. Mackensen (2010), The tropical rainbelt and productivity changes off northwest Africa: A 31,000-year high-resolution record, *Mar. Micropaleontol.*, *76*(3-4), 76–91, doi:10.1016/j.marmicro.2010.06.001.

Zarriess, M., and A. Mackensen (2011), Testing the impact of seasonal phytodetritus deposition on $\delta^{13}C$ of epibenthic foraminifer *Cibicidoides wuellerstorfi*: A 31,000 year high-resolution record from the northwest African continental slope, *Paleoceanography*, *26*(2), PA2202, doi:10.1029/2010PA001944.

Zarriess, M., H. Johnstone, M. Prange, S. Steph, J. Groeneveld, S. Mulitza, and A. Mackensen (2011), Bipolar seesaw in the northeastern tropical Atlantic during Heinrich stadials, *Geophys. Res. Lett.*, *38*(4), L04706, doi:10.1029/2010GL046070.